Forty-thousand years of maritime subsistence near a changing shoreline on Alor Island (Indonesia)

Shimona Kealy [a, b, c, *], Sue O'Connor [a, b], Mahirta [d], Devi Mustika Sari [d], Ceri Shipton [a, b, e], Michelle C. Langley [f, g], Clara Boulanger [a, b, h], Hendri A.F. Kaharudin [d, i], Esa P.B.G.G. Patridina [d], Muhammad Abizar Algifary [d], Abdillah Irfan [d], Phillip Beaumont [a], Nathan Jankowski [j, k], Stuart Hawkins [a, b], Julien Louys [f]

[a] Archaeology and Natural History, School of Culture, History and Language, College of Asia and the Pacific, Australian National University, Canberra, ACT, Australia
[b] ARC Centre of Excellence for Australian Biodiversity and Heritage, Australian National University, Canberra, ACT, Australia
[c] Evolution of Cultural Diversity Initiative, Australian National University. Canberra, ACT, Australia
[d] Departemen Arkeologi, Fakultas Ilmu Budaya, Universitas Gadjah Mada, Yogyakarta, Indonesia
[e] Institute of Archaeology, Gordon Square, University College London, London, UK
[f] Australian Research Centre for Human Evolution, Environmental Futures Research Institute, Griffith University, Brisbane, QLD, Australia
[g] Forensics and Archaeology, School of Environment and Science, Griffith University, Brisbane, QLD, Australia
[h] Muséum National d'Histoire Naturelle, UMR 7194 Histoire Naturelle de l'Homme Préhistorique, Paris, France
[i] School of Archaeology and Anthropology, College of Arts and Social Science, Australian National University, Canberra, ACT, Australia
[j] Centre for Archaeological Science, School of Earth, Atmospheric and Life Sciences, University of Wollongong, Wollongong, NSW, Australia
[k] ARC Centre of Excellence for Australian Biodiversity and Heritage, University of Wollongong, Wollongong, NSW, Australia

ARTICLE INFO

ABSTRACT

We report archaeological findings from a significant new cave site on Alor Island, Indonesia, with an *in situ* basal date of 40,208−38,454 cal BP. Twenty thousand years older than the earliest Pleistocene site previously known from this island, Makpan retains dense midden deposits of marine shell, fish bone, urchin and crab remains, but few terrestrial species; demonstrating that protein requirements over this time were met almost exclusively from the sea. The dates for initial occupation at Makpan indicate that once *Homo sapiens* moved into southern Wallacea, settlement of the larger islands in the archipelago occurred rapidly. However, the Makpan sequence also suggests that the use of the cave following initial human arrival was sporadic prior to the terminal Pleistocene about 14,000 years ago, when occupation became intensive, culminating in the formation of a midden. Like the coastal sites on the larger neighbouring island of Timor, the Makpan assemblage shows that maritime technology in the Pleistocene was highly developed in this region. The Makpan assemblage also contains a range of distinctive personal ornaments made on *Nautilus* shell, which are shared with sites located on Timor and Kisar supporting connectivity between islands from at least the terminal Pleistocene. Makpan's early inhabitants responded to sea-level change by altering the way they used both the site and local resources. Marine food exploitation shows an initial emphasis on sea-urchins, followed by a subsistence switch to molluscs, barnacles, and fish in the dense middle part of the sequence, with crabs well represented in the later occupation. This new record provides further insights into early modern human movements and patterns of occupation between the islands of eastern Nusa Tenggara from ca. 40 ka.

© 2020 The Authors. Published by Elsevier Ltd. This is an open access article under the CC BY license (http://creativecommons.org/licenses/by/4.0/).

1. Introduction

Recent modelling efforts strongly support a northern landing for the initial arrival of humans on Sahul from the islands of Wallacea (Kealy et al., 2017, 2018; Norman et al., 2018, Bird et al., 2019). A southern route for initial dispersal is considered less likely, and the

* Corresponding author. Archaeology and Natural History, School of Culture, History and Language, College of Asia and the Pacific, Australian National University, Canberra, ACT, Australia.
E-mail address: shimona.kealy@anu.edu.au (S. Kealy).

earliest dates of *Homo sapiens* on the islands of Nusa Tenggara (Fig. 1) do not dispute these models. They do, however, support the hypothesis that following initial arrival on Sahul, early humans continued to disperse throughout Wallacea, possibly using the southern route to Sahul at a later time (Kealy et al., 2018; Norman et al., 2018; Bradshaw et al., 2019).

On Flores, at the site of Liang Bua, early occupation by *Homo floresiensis* is overlain by deposits bearing the remains of *H. sapiens* (Morwood et al., 2009; Sutikna et al., 2018). Based on changes in stone tool materials, Sutikna et al. (2018) argued that *H. sapiens* had arrived on Flores by ca. 47.7—44.1 ka cal BP. To the east and south of Flores, the island of Timor has produced several sites where occupation records overlap with the early *H. sapiens* occupation of Liang Bua (Hawkins et al., 2017; Sutikna et al., 2018; Shipton et al., 2019), in particular Asitau Kuru (previously known as Jerimalai) with an initial occupation dated to 46.5—43.1 ka cal BP (Shipton et al., 2019). The archaeological records from these two islands suggest that *H. sapiens* was well established throughout the eastern Nusa Tenggara islands by ca. 44 ka.

In addition to the northern Australian site of Madjedbebe, which suggests a human arrival date on Sahul as early as ca. 65 ka (Clarkson et al., 2017), a multitude of different records strongly support human dispersal across Australia prior to 50 ka (Turney et al., 2001; Bird et al., 2002; Bowler et al., 2003; Hamm et al., 2016; Wood et al., 2016; Delannoy et al., 2017; Tobler et al., 2017; Veth et al., 2017; Maloney et al., 2018a). The more recent dates for *H. sapiens* occupation in Flores and Timor may therefore represent a later dispersal into the southern Wallacean islands at ca. 45 ka, following the initial dispersal event(s) into northern Wallacea and then Sahul, prior to 50 ka (Kealy et al., 2018; Norman et al., 2018).

Alor lies between the islands of Flores and Timor. This location makes it a logical 'stepping-stone' on any southern migratory pathway for dispersal of *H. sapiens* (Fig. 1; Kealy et al., 2016, 2018; O'Connor et al., 2017a). The only archaeological site hitherto investigated on Alor, Tron Bon Lei, recorded human occupation back to just 21 ka cal BP, beneath which bedrock was encountered (Samper Carro et al., 2016a, 2017, 2019). This result was in contrast with the nearby islands of Flores and Timor with records for *H. sapiens* occupation extending back at least another 20,000 years (Sutikna et al., 2018; Shipton et al., 2019). In discussing the settlement chronology for Tron Bon Lei, O'Connor et al., 2017a suggested that the dates might indicate that only the larger islands of the Nusa Tenggara (Lesser Sunda) chain such as Flores and Timor were occupied by ca. 45 ka. They hypothesised that intermediate and smaller-sized islands, such as Alor, may only have been first settled during the lowered sea stand of the Last Glacial Maximum (LGM) (ca. 22—21 ka) when they merged with neighbouring islands to create mega-islands more similar in size to Flores and Timor (O'Connor et al., 2017a: Figs. 4 and 5).

However, research on very small islands such as Kisar has shown that colonisation and (at least temporary) occupation of islands is not solely dependent on the extent of land mass (O'Connor et al., 2019). As models of coastal adaptation have suggested, the rich near-shore resources of the Nusa Tenggara Archipelago would have provided early communities with a subsistence strategy that had low dependency on terrestrial resources (Allen and O'Connell, 2008; O'Connell and Allen, 2012; Fitzpatrick et al., 2016; O'Connor et al., 2019). Coastal ecosystems have been identified as
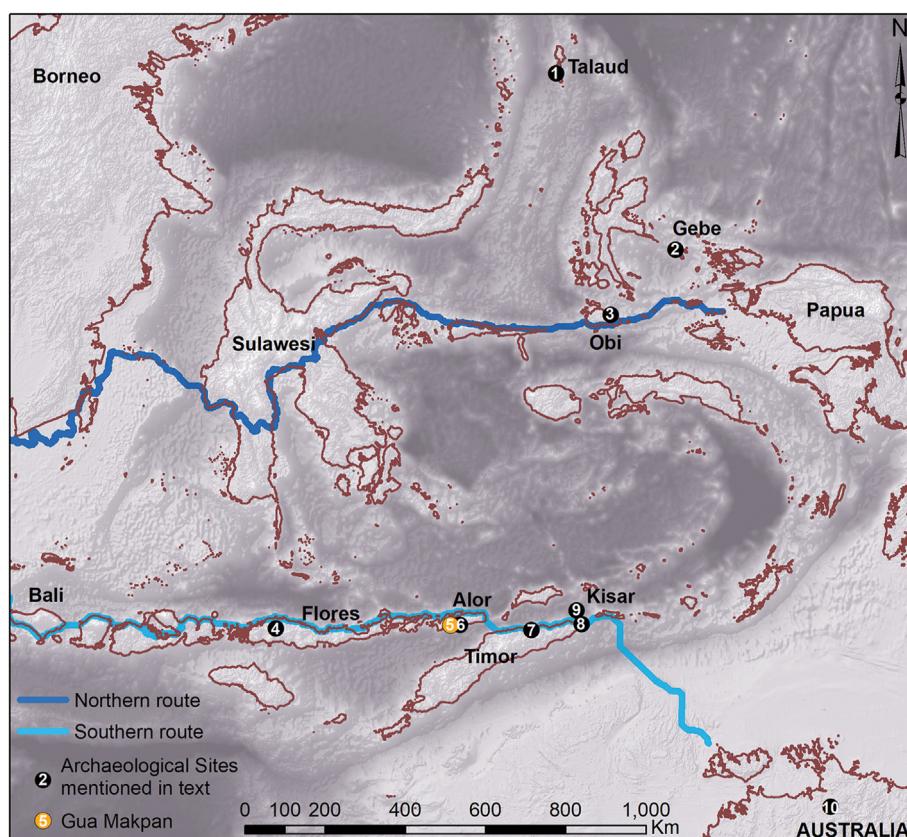
Fig. 1. Map of the region showing the location of Alor island and the site of Makpan (#5 — orange circle). Other sites mentioned in the text are marked with black circles. Numbers corresponding to the following sites: 1) Liang Sarru; 2) Golo Cave; 3) Kelo 2 & Kelo 6; 4) Liang Bua; 6) Tron Bon Lei; 7) Laili; 8) Asitau Kuru; 9) Here Sorot Entapa; 10) Madjedbebe. Least-cost pathway model routes from Sunda to Sahul are shown following Kealy et al. (2018). (For interpretation of the references to colour in this figure legend, the reader is referred to the Web version of this article.)

zones with a high abundance of resources that maximise energy intake (i.e. consumption of food) over energy output (i.e. time/effort spent hunting/foraging) (Szabó and Amesbury, 2011; O'Connell and Allen, 2012; Fitzpatrick et al., 2016), making them attractive for human occupation irrespective of island size.

Theories of intensive coastal exploitation were also explored by researchers such as Clark (1991) who suggested that such a subsistence focus, and the maritime technologies and capabilities it would have required, promoted the rapid colonisation of the Wallacean islands. The more abundant resources of unexploited shores would have been attractive to neighbouring communities, encouraging frequent movement (Allen and O'Connell, 2008). As population density increases at a certain location, more and more members of the community would be motivated to explore for pristine shores, perhaps leading to the occasional overnight stay on neighbouring islands, which could slowly evolve into temporary or seasonal camps, if not permanent settlements. A better understanding of how these coastal resources were used, the technical capabilities of these early communities, and how they responded to other influencing factors such as sea-level change, is required to examine and refine this theory of human dispersal.

Here we report archaeological results from a significant new cave site on Alor Island known as Gua Makpan (hereafter: Makpan). The new sequence from Makpan enables the exploration of various scenarios of early modern human movements and patterns of occupation between the islands of eastern Nusa Tenggara from ca. 40 ka. The Makpan sequence is used to examine how early Alor communities responded to changes in sea levels and coastal topography.

2. Materials and methods

2.1. Background and excavation of Makpan

Alor Island is volcanic in origin and comprised of a steep, rocky, and stepped interior, with a narrow coastal margin (Koesoemadinata and Noya, 1989; Reepmeyer et al., 2016). Makpan is located in the Alor Formation which is characterised by fine-grained, dark-to-light grey basaltic to andesitic volcanics estimated to be Late Miocene to Early Pliocene in age. It comprises the majority of the island's geology (Koesoemadinata and Noya, 1989). While today Alor has a total land area of 2119 km^2, during the LGM it was merged with adjacent islands Pantar, Pura, Marisa, Rusa, Ternate, Treweng Kangge, and Kambing; forming a substantially larger island of about 3860 km^2 (O'Connor et al., 2017a).

Makpan was located during reconnaissance of Alor Island in 2015 and excavated in June and July 2016 by a joint team from the Australian National University and Universitas Gadjah Mada. It is a large, spacious lava tube cave on the southwest coast between the modern villages of Halmin and Ling Al (Figs. 2 and 3). The name "Makpan" means "echo" in the local language, reflecting the cave's large size. The cave entrance faces the ocean, and is today ~386 m from the shoreline and ~37.5 m above current mean sea level (Fig. 3A). Even during sea-level minima, Makpan would have been within walking distance of the coast as the offshore topography in this region drops away steeply to a depth of −100 m, less than 1.8 km off the current shoreline (Fig. 4).

The 2016 season consisted of two separate excavations: the 'main' 2 × 2 m excavation (comprising squares A, B, C and D; see Fig. 3G) in the centre-front portion of the cave, targeting the human occupation record, and a second single 1 × 1 m square deeper within the cave and situated directly below a modern-day owl roost in order to target a sample of non-anthropogenic fauna (Fig. 3C). The owl roost pit was excavated to a maximum depth of 1 m with
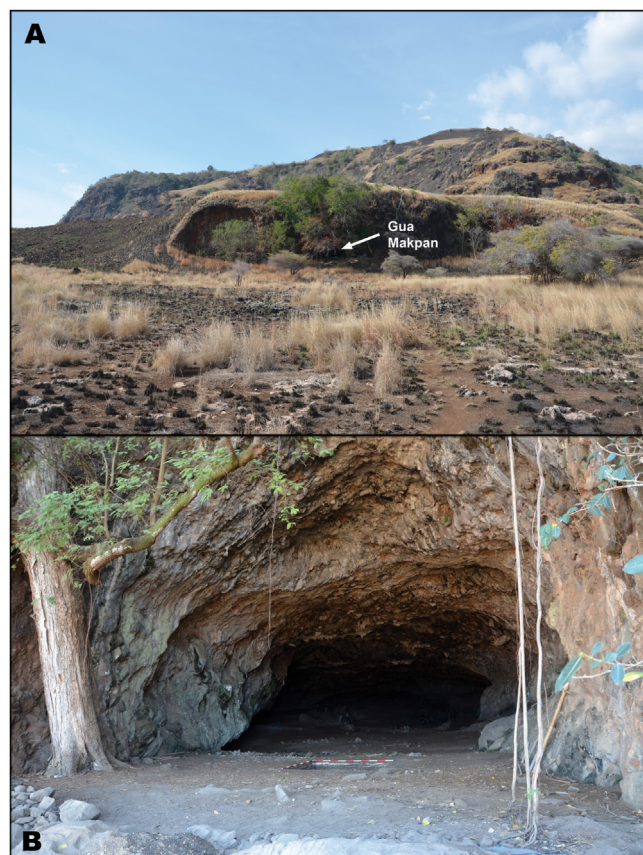

Fig. 2. The archaeological site of Gua Makpan. A) Overview photo (facing north) of the cave mouth. B) The 'main pit' archaeological excavation.

the lowest layer dated to ca. 7.9−7.6 ka cal BP (see Louys et al., 2018). From here on we refer only to the 'main' excavation of Makpan.

The main (2 m^2) excavation was opened near the cave entrance, but well inside the dripline (Figs. 2 and 3). Excavation was carried out in spits of ~5 cm thickness within stratigraphic layers. All excavated material was dry screened through 1.5 mm mesh and subsequently wet screened at the same scale, before drying and sorting, ensuring good recovery of small finds including lithic micro-debitage, fish bone, sea urchin spines, and shell artefacts. Following the completion of spit 23 and at a depth of ~1.5 m, the pit was shored and excavation continued in only a single 1 × 1 m square: square B. Excavation of square B (down to spit 68) reached an additional ~2 m, making a maximum total excavation depth of 3.5 m. Excavation of square B was halted when culturally sterile cemented sand, which was presumed to represent the base of the occupation deposit, was reached.

2.2. Bathymetric modelling

Modern bathymetric data for the Alor Archipelago and the Ombai Strait which separates it from Timor to the south, was obtained from the General Bathymetric Chart of the Oceans (GEBCO_19) dataset (Smith and Sandwell, 1997). This bathymetric data indicates a relatively steep drop-off along Alor's south coast into the Ombai Strait, but a shallowly submerged shelf connecting Alor island with Pantar to the west. In order to reconstruct the past coastline and near-shore environmental conditions adjacent to Makpan we used the GEBCO_19 dataset, in addition to palaeosea-
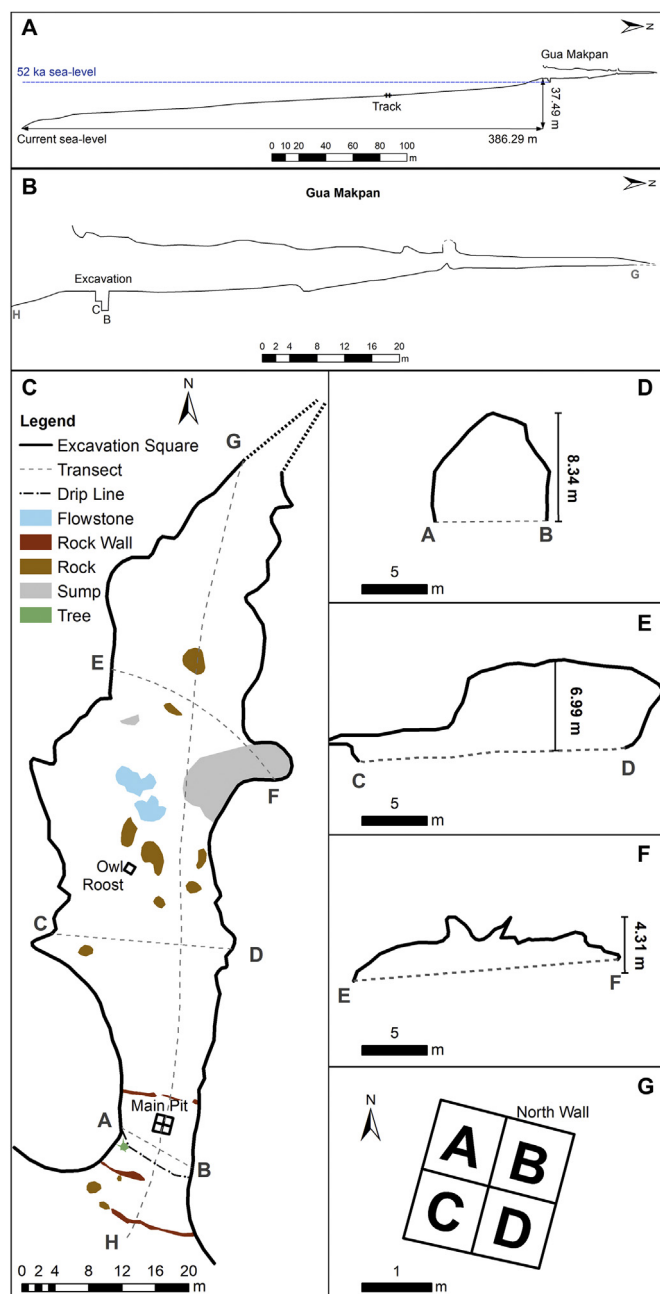
Fig. 3. Plan and transects of Gua Makpan. A) Vertical transect from the present coastline to Makpan. B) Vertical transect of Makpan, crosscutting the excavation, corresponding to the G-H line on the plan (C). C) Cave plan. D) Horizontal transect of cave mouth corresponding to A-B line on the plan. E) Horizontal transect of cave centre corresponding to C-D line on the plan. F) Horizontal transect of back of cave corresponding to E-F line on the plan. G) Layout of the Makpan main pit and division into the four 1 × 1 m excavation squares.

level data (Lambeck and Chappell, 2001), and local uplift estimates (Hantoro et al., 1994; this study). The Lambeck and Chappell (2001) sea-level model was selected as it is the most recent sea-level model for the region which informs on the last 40 ka. For the rate of uplift we used both the rate of 1.2 m/ka obtained by Hantoro et al. (1994) for the north coast of Alor, and a new rate calculated here based on the age of the sterile sand layer at the base of the Makpan excavation (see below). Relative sea level for the last 40 ka in the Alor Archipelago was calculated following the methodology of Kealy et al. (2017, 2018). Palaeo-island extent and topography were

then modelled (Kealy et al., 2018) at key periods during the human occupation of Makpan (Fig. 4).

2.3. Radiocarbon calibration and bayesian model

All radiocarbon dates in this paper are calibrated using OxCal v. 4.4 (Ramsey, 2009a) to 95.4% probability, using the IntCal20 (for charcoal and tooth enamel; Reimer et al., 2020) and Marine20 (for marine shell; Heaton et al., 2020) calibration curves. Marine shell dates are calibrated without ΔR as this data is currently unavailable for Alor and the few known local reservoir effects from the wider region cover a range of less than ±100 years (Southon et al., 2002), so would not appreciably alter the millennial scale patterns reported here.

Samples were taken to test the field interpretation that the sand at the base of the sequence represented deposition by a shoreline beach, rather than non-marine origin, or a catastrophic event. Geophysical, geochronological, and thin section analysis of the basal sterile layer was conducted on a large (20 cm³) oriented semi-consolidated block sample recovered from the north-west quadrant of spit 68 in square B (B68). A sub-sample of B68 sediment was crushed and sieved through a 63 μm sieve and shell and coral fragments selected on the basis of minimal wear, rounding, and identifiable features. These were submitted to the Waikato Radiocarbon Laboratory (Wk) for dating.

In addition to the sterile sand layer, 50 radiocarbon samples (charcoal = 28, marine shell = 21, bone = 1) obtained from the Makpan excavation were dated by the Australian National University Radiocarbon Dating Centre (ANU; Table 1). Twenty samples were collected *in situ* during excavation and their 3D position recorded, while thirteen *in situ* samples were also collected from the walls at the completion of the excavation, and their position within the stratigraphy noted (Figs. 5 and 6). Four of these samples pertain to the burial in layer 5; three on charcoal from associated sediments, and one a direct date on the burial from tooth enamel (see Samper Carro et al. forthcoming, for a detailed report on the burial). While the 3D position of four other samples collected from the excavation is uncertain, their association with assigned spits and layers is considered reliable as they were recovered during the excavation process.

Following the completion of the excavation, thirteen additional samples were selected for dating from the partially analysed shell assemblage in an attempt to broaden the coverage of dates across the majority of excavated spits. The lack of *in situ* information for these 13 additional samples, however, makes their contextual associations less reliable than the Makpan radiocarbon samples collected during excavation. One of these samples, (ANU 53611), was later rejected as a definite outlier as preliminary concern about this specimen's association with spit 66 (slight differences in soil matrix colouration) was supported by the significantly younger radiocarbon date than others obtained from the same layer. We therefore consider radiocarbon sample ANU 53611 to have been displaced due to contamination from higher layers (i.e. the relatively unstable midden deposit of layer 10) during (or possibly after) excavation.

The identification of these non-*in situ* specimens as marine shells (in a volcanic cave well above the high-tide mark), in addition to properties of their preservation and fragmentation, means we can be confident that these shells were brought into Makpan by people. Thus, the 12 remaining non-*in situ* samples, despite uncertainty surrounding their exact stratigraphic association, are still dates directly associated with human occupation at the site and are retained in our study. In total 49 radiocarbon dates are reported for the Makpan assemblage.

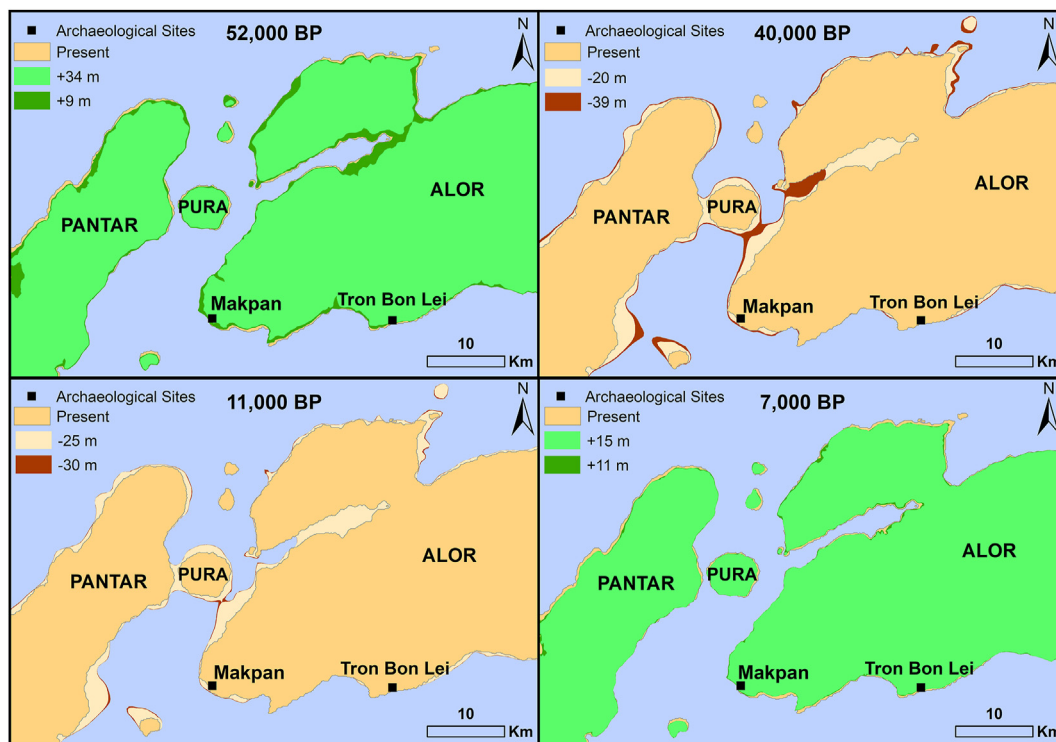A multiphase Bayesian model was constructed using these dates

Fig. 4. Palaeogeographic reconstructions of western Alor and the Pantar Strait showing reconstructions based on both the Hantoro et al. (1994) uplift rate (darker shading) and the Makpan uplift rate (lighter shading) following Fig. 7 reconstructions from left to right are: ca. 52 ka, ca. 40 ka, ca. 11 ka, and ca. 7 ka.

in OxCal v. 4.4 (Ramsey, 2009a, 2017) to reduce the uncertainty of the age estimates and to predict the timing of the transitions between different identified phases. All 49 radiocarbon dates were included in the model. The General t-type Outlier Model (Ramsey, 2009b) and a prior outlier probability of 5% was applied to the overall model and each individual date, respectively. This model is the one most commonly used for archaeological dates in determining the probabilities of outliers and the scale of offset applied to the data within the model (Ramsey, 2009b; Wood et al., 2016). The exception to this 5% outlier probability was for the 13 non-*in situ* samples. As these were considered to be less reliable with regards to their stratigraphic associations, and thus significantly more likely to be outliers, we applied a prior outlier probability of 50% to these dates.

The Difference Function in OxCal v. 4.4 was then used to examine the continuity in the radiocarbon record between the five phases and detect the presence of any discontinuities (i.e. hiatus) at 95.4% probability (Wood et al., 2016). This function subtracts one probability distribution function from another. If zero is included in the probability range, the probability distribution functions are regarded as indistinguishable at 95.4%. Thus, the modelled distribution for the start of phase 2 was subtracted from the modelled distribution of the end of phase 1, the start of phase 3 was subtracted from the end of phase 2, and so forth.

2.4. Analysis of cultural materials

Here we focused only on square B of the excavation as it is the only square for which a complete sequence of the deposit has so far been obtained. Materials recovered from square B included a variety of cultural artefacts (i.e. lithics, shell artefacts, pottery) and zooarchaeological remains (i.e. vertebrate and invertebrate fauna). We provide a broad description of these remains here based on general and preliminary investigations, with specialised analyses to

be presented in forthcoming publications. Overall counts and weights of the various materials were compared based on both their 'raw' values as well as values adjusted for the total excavated volume of the corresponding spit following Kaharudin et al. (2019:538). Our preliminary analysis of the faunal assemblages identified very low rates of calcium carbonate precipitation or cementation on specimens. As such, we are confident the faunal weights are a 'true' representation of the material recovered from the site. Additionally, by separating this material into taxonomically similar categories, relative comparisons between phases but within groups allow a reasonable assessment of taxonomic abundance over time.

2.4.1. Stone artefact analysis

Three categories of stone artefacts were recovered from square B: flaked artefacts, cobble manuports, and grinding stones and anvils. For the stone flaked artefacts, the total number of artefacts (TNA) count was further subdivided based on material type.

2.4.2. Shell and coral artefacts

Non-lithic artefacts recovered from the square B excavation were identified based on raw material, form, and degree of completion. These artefacts were examined for taphonomic and anthropogenic alterations, grouped according to type, and their total number for each spit recorded. 'Tools' were identified based on evidence for shaping/manufacture (e.g. flaking, grinding) and use wear.

2.4.3. Pottery analysis

The distribution of plain, decorated and slipped pottery sherds recovered from square B were recorded and separated according to the part of the vessel from which they derived.

Table 1
Radiocarbon samples analysed from Makpan. Calibrated and modelled in OxCal v.4.4 (Ramsey, 2009a) using the IntCal20 (for charcoal and tooth enamel; Reimer et al., 2020) and Marine20 (for shells; Heaton et al., 2020) calibration curves. Unmodelled and modelled calibrated dates are all shown at 95.4% posterior probability. Spits and Layers correspond to the stratigraphy (see Figs. 5 and 6), the date model is shown in Fig. 7. See also Supplementary Table S1.

Phase	ID	Sample name	Spit	Layer	Sample type (species)	^{14}C Date ± error	Calibrated Date (2σ) BP	Modelled Date (2σ) BP
P5	ANU 52323	MPA1	1	1	Charcoal	518 ± 23	553–510	622–507
	ANU 51814	MP_Wall1	1	2	Charcoal	714 ± 30	716–564	721–558
	ANU 52311	MP_Wall3	2	2	Charcoal	1018 ± 24	960–829	2128–827
	ANU 51816	MP_Wall2	3	2	Charcoal	1214 ± 28	1248–1061	1272–892
	ANU 52312	MP_Wall4	6	4	Charcoal	2287 ± 26	2352–2160	2518–2159
	ANU 52332	MPD6-10	6	4	Charcoal	2241 ± 28	2338–2153	2337–2152
	ANU 52313	MP_Wall6	9	4	Charcoal	3087 ± 25	3370–3225	3388–3225
P4	ANU 52314	MP_Wall7	10	5	Charcoal	6775 ± 29	7670–7579	7671–7580
	ANU 56516	MP Burial	11	5	Tooth enamel (*Homo sapiens*)	7041 ± 36	7957–7788	7959–7787
	ANU 52324	MPA11	11	5	Charcoal	7314 ± 29	8179–8030	8180–8028
	ANU 52333	MPD11-20	11	5	Charcoal	7515 ± 30	8390–8206	8392–8199
	ANU 51606	MP_Wall8	13	5	Shell (*Turbo* sp.)	7867 ± 33	8310–8005	8324–8002
	ANU 53911	MP_burial_2	13	5	Charcoal	7936 ± 32	8985–8637	8985–8608
	ANU 52316	MP_Wall9	16	6	Charcoal	7945 ± 30	8984–8643	8986–8643
	ANU 52334	MPD18251	18	6	Charcoal	8959 ± 35	10,226 - 9914	10,220 - 9911
	ANU 52335	MPD18252	18	6	Charcoal	8952 ± 35	10,222 - 9913	10,212 - 9911
	ANU 53622	MPB20	20	7	Shell (Muricidae)	9298 ± 41	10,135 - 9702	10,913 - 8889
P3	ANU 52317	MP_Wall12	21	10	Charcoal	10,050 ± 34	11,802–11,351	11,750–11,353
	ANU 51613	MPD24311	24	10	Shell (*Patella* sp.)	10,251 ± 42	11,395–11,055	11,735–11,096
	ANU 52336	MPD24312	24	10	Charcoal	10,091 ± 38	11,822–11,402	11,815–11,401
	ANU 52318	MP_Wall14	25	10	Charcoal	10,073 ± 34	11,811–11,401	11,804–11,400
	ANU 51607	MP_Wall15	28	10	Marine Shell (unknown species)	10,244 ± 38	11,382–11,059	11,735–11,105
	ANU 52325	MPB29A75	29	10	Charcoal	10,055 ± 34	11,805–11,355	11,752–11,355
	ANU 51410	MPB30-35	30	10	Charcoal	10,100 ± 38	11,829–11,402	11,819–11,401
	ANU 52321	MPB_North-S7	31	10	Charcoal	10,118 ± 38	11,928–11,404	11,831–11,402
	ANU 52326	MPB32-36	32	10	Charcoal	10,162 ± 35	11,939–11,648	11,927–11,402
	ANU 52320	MPB_North-S1	33	13	Charcoal	10,087 ± 34	11,818–11,402	11,811–11,402
	ANU 53621	MPB35	35	15	Shell (*Tridacna* sp.)	10,483 ± 45	11,776–11,296	11,790–11,273
P2	ANU 53620	MPB37	37	17	Shell (Muricidae)	11,842 ± 52	13,333–12,994	13,638–12,012
	ANU 52327	MPB38-39	38	17	Charcoal	10,552 ± 37	12,685–12,481	13,200–12,471
	ANU 51411	MPB39-50	39	17	Charcoal	10,556 ± 39	12,689–12,481	12,692–12,479
	ANU 51610	MPB_NW_1	42	17	Shell (*Haliotis* sp.)	10,903 ± 45	12,450–11,958	12,472–11,964
	ANU 51611	MPB42-1	42	17	Shell (*Patella* sp.)	10,957 ± 41	12,490–12,025	12,509–12,060
	ANU 52329	MPB42-2	42	17	Charcoal	10,445 ± 35	12,612–12,102	12,613–12,104
	ANU 52330	MPB45-51	45	17	Charcoal	11,609 ± 37	13,581–13,356	13,580–13,354
	ANU 51416	MPB47-1	47	17	Shell (*Patella* sp.)	11,003 ± 42	12,569–12,104	12,590–12,116
	ANU 52331	MPB48	48	17	Charcoal	10,567 ± 35	12,691–12,485	12,696–12,485
	ANU 51612	MPB49-1	49	17	Shell (*Patella* sp.)	12,237 ± 43	13,760–13,414	13,757–13,382
	ANU 53619	MPB50	50	17	Shell (Muricidae)	10,389 ± 42	11,625–11,201	13,595–11,508
	ANU 53618	MPB51	51	17	Shell (Muricidae)	10,143 ± 46	11,243–10,854	13,458–11,492
	ANU 53617	MPB52	52	17	Shell (Muricidae)	11,649 ± 48	13,123–12,787	13,574–12,292
	ANU 53616	MPB53	53	17	Shell (Muricidae)	11,821 ± 48	13,309–12,976	13,898–12,278
	ANU 53614	MPB54	54	17	Shell (Muricidae)	13,138 ± 50	15,208–14,680	15,028–12,124
	ANU 53613	MPB57	57	17	Shell (Muricidae)	11,783 ± 48	13,276–12,930	13,667–12,658
P1	ANU 51412	MPB61-56	61	18	Charcoal	17,893 ± 69	21,993–21,440	22,007–21,440
	ANU 51417	MPB62-58	62	18	Shell (*Patella* sp.)	35,130 ± 414	40,241–38,453	40,514–38,105
	ANU 53612	MPB64	64	18	Shell (Muricidae)	13,177 ± 51	15,250–14,780	16,473–14,088
	ANU 53610	MPB67	67	18	Shell (*Asaphis violascens*)	19,894 ± 87	23,316–22,731	24,603–21,263
	ANU 53609	MPB68	68	18	Shell (*Turbo* sp.)	35,232 ± 427	40,360–38,585	44,533–37,823

2.4.4. Vertebrate fauna analysis

The vertebrate faunal assemblage from square B was sorted into two categories: fish (both cartilaginous and bony fishes) and tetrapods. Tetrapods were then further sub-divided by general size into micro- (<180 g) and macro- (>180 g) size categories. This subdivision was based on the upper weight limit for common owl prey in the region (Olsen et al., 2020) and the study by Hawkins et al. (2018) from nearby Tron Bon Lei (TBL) that identified barn owls *Tyto alba* as the primary accumulators of the microvertebrate tetrapod remains recovered in the TBL archaeological assemblage. Makpan is a prime habitat for barn owl roosts and preserves evidence of their presence from both prehistoric and modern times (Louys et al., 2018), with a single barn owl observed roosting in the cave during the excavation period.

Following Hawkins et al. (2018) and Olsen et al. (2020), we separated giant rats, fruit bats, and turtles into the macrovertebrate (anthropogenic) classification and all other tetrapods (e.g. small-medium rodents, microbats, lizards, snakes, small birds, etc) into the microvertebrate (likely owl roost deposit) category. The only exceptions, emphasised by our weight division at ~180 g, was the inclusion of small fruit bats (Hawkins et al., 2018; Olsen et al., 2020) and juvenile giant rats (Louys et al., 2018) within the smaller (<180 g) microvertebrate category.

Bone weights for these vertebrate groups were documented per spit. Common taxonomic groups (e.g. rat, tuna, etc) noted during initial sorting of the vertebrate material is recorded here in addition to the results of preliminary taxonomic analysis of the fish remains for four spits in phase 3, to provide further detail on the species diversity present in this assemblage. Phase 3 is the midden phase which recovered the greatest record of marine exploitation at Makpan (including fish remains), and so was the focus of this preliminary sample of taxonomic diversity.
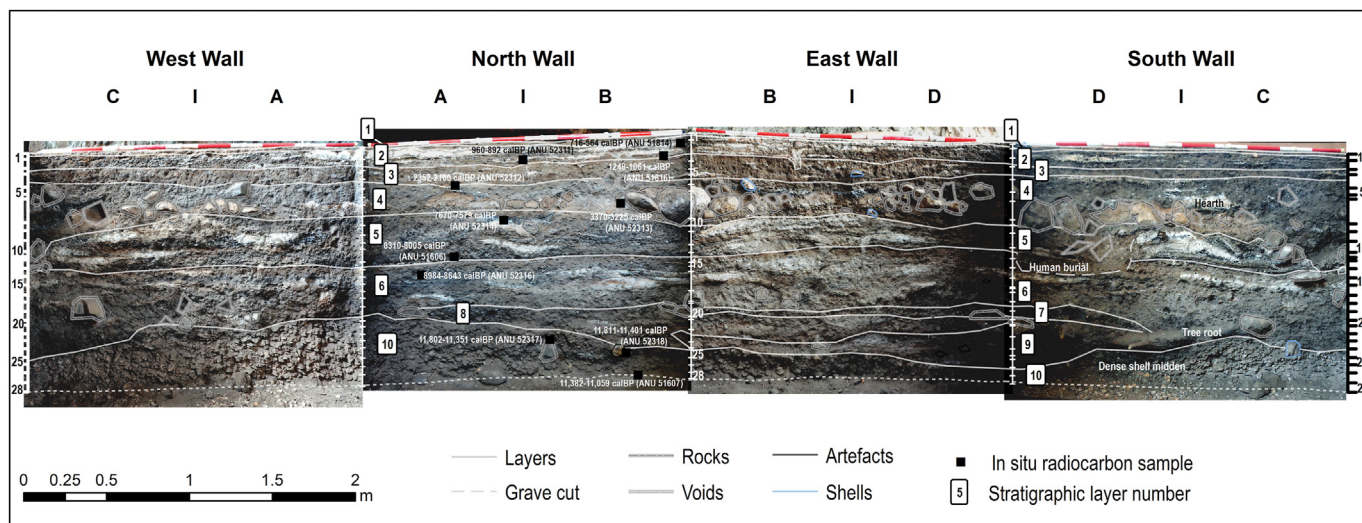
Fig. 5. Stratigraphic section of the upper 2 × 2 m excavation at Makpan. White lines delineate stratigraphic layers and are numbered accordingly.
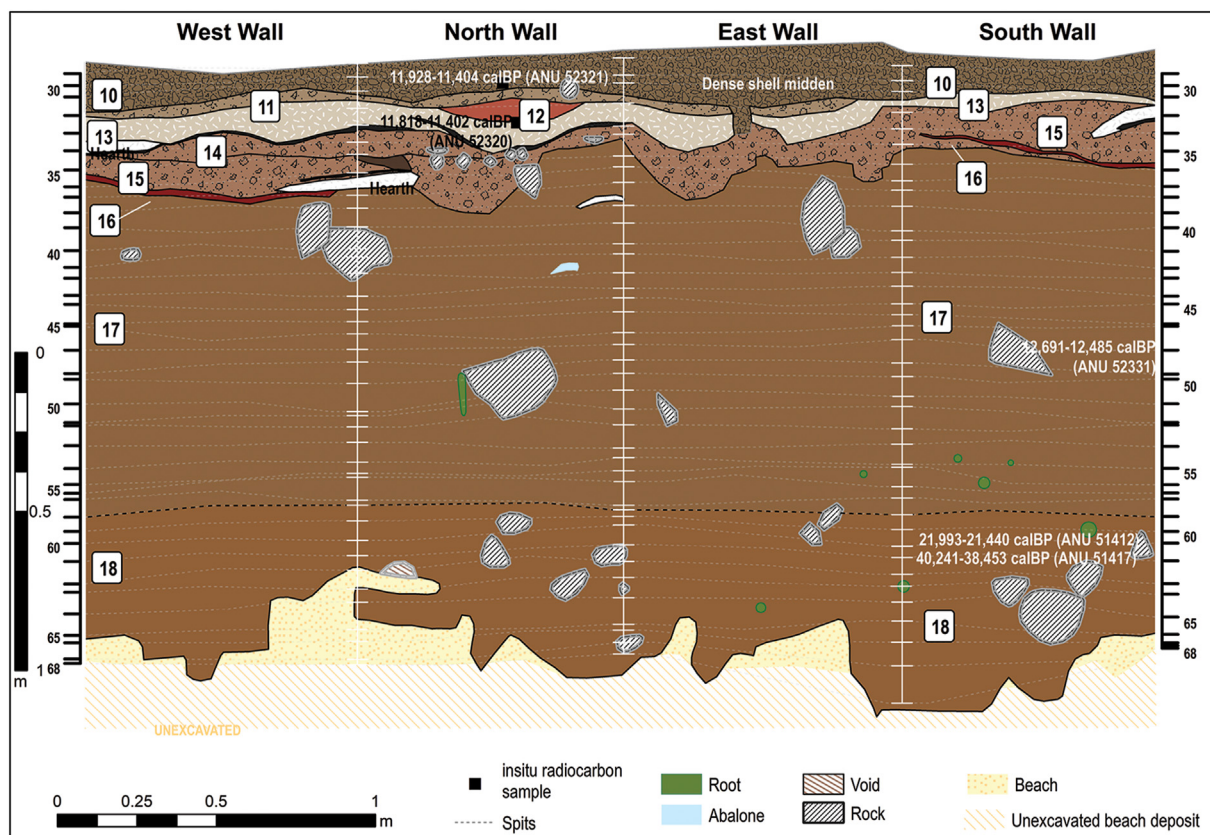

Fig. 6. Stratigraphic section of the lower 1 × 1 m square B excavation at Makpan. Stratigraphic layers are numbered and spits indicated by dotted lines.

2.4.5. Invertebrate fauna analysis

The invertebrate faunal assemblage recovered from square B was sorted into four groups: shell (Mollusca), barnacles (Arthropoda: Cirripedia), crabs (and lobsters; Arthropoda: Decapoda), and sea urchins (Echinodermata: Echinoidea). Weights per spit were recorded for each group. As for the fish, preliminary species-level analysis of the shells and urchins is reported for selected spits to demonstrate the range of taxa.

3. Results

3.1. Makpan chronostratigraphic sequence

3.1.1. Makpan stratigraphy

A total of 18 cultural layers were identified from the Makpan excavation based on various geological characteristics of the sedimentary grains including their size, sorting, morphology, fabric,

inclusions, compaction, and colour (Figs. 5 and 6). The soft topsoil of moderately-well sorted sandy silt was counted as layer 1 and excavated in a single spit. Below this, layer 2 was characterised by a moderately-well sorted, friable sandy silt of a dark brown colour (7.5 YR 3/2) with multiple, thin ash lenses dispersed throughout — suggestive of frequent small hearths. Layer 3 is a little darker (7.5 YR 2.5/3), with a moderately sorted mix of sandy silt and silty sand, distinct from the preceding layer for the reduction in ash/hearths.

Distinguished by a sudden increase in rocks of various sizes, layer 4 is particularly poorly sorted with a dark grey (7.5 YR 4/1) sandy silt matrix. Horizontally bedded, the rocks of layer 4 are thought to have an anthropogenic origin, supported by the density of their placement, and the use of different sized rocks to form a connected feature that may have been a rock floor. Interestingly, this rock floor layer also directly overlies the human burial which has been dug into layer 5 (Fig. 5; Samper Carro et al. forthcoming). Layer 5 is distinct for the significant increase in hearths, preserved as multiple ash and charcoal lenses of varying thickness in a surrounding very dark grey (7.6 YR 3/1) sandy silt matrix, moderately-poorly sorted with shell fragments and gravel inclusions. Similar to layer 5, layer 6 is distinguished by having fewer and thinner ash lenses, less charcoal and shell fragments, a finer moderately sorted dark to very dark grey (7.5 YR 5—4/1) matrix, and a slight increase in rock and cobble inclusions. Layer 7 is a very dark brown-black (7.5 YR 2.5/1—2) thin layer which is not apparent across the entirety of the excavation. Similarly, layers 8 and 9 were only observed across part of the excavation, despite being thicker than layer 7. Both layers 8 and 9 are distinguished by an increase in small and large roots and a return to the dark grey (7.5 YR 5/1) colour of layer 6. Layer 9 preserves a greater abundance of ash than layer 8.

Layer 10 is a dense shell midden layer, preserving an abundance of both whole and fragmented shells in a brown (7.5 YR 4/2) silty sand, ash-rich matrix. The base of the thick layer 10 is characterised by a series of thinner layers (11—16) preserving the distinct remains of hearth activity such as ash lenses and burnt sediments. Layer 11 is the most shell-rich of these layers, although significantly less dense than the overlying shell midden of layer 10. The matrix of layer 11 is a relatively loose brown (7.5 YR 5/2—3) silty sand. Layer 12 is a thick lens of reddish-dark brown (7.5 YR 3/3) sediment whose colouration and compaction are clearly the result of burning. This layer was not observed throughout the entirely of the section (Fig. 6) but did extend somewhat into the plan of the excavation. Below layers 11 and 12, layer 13 is an extremely ash-rich, light grey (7.5 YR 7/1) layer with substantial compaction, particularly in the lower two-thirds of the layer, with thin lenses of burnt sediment and some distinct hearths occurring along the base. Layers 14 and 15 are also shell midden layers although less dense in shell than layer 10 and with a greater abundance of ash and hearth features. With a matrix of reddish-brown (7.5 YR 5—4/2) sandy silt, the key distinguishing features between layer 14 and 15 are the occurrence of some crystalline precipitates on a number of the shells in layer 14, and a slight reduction in shell density in layer 15. Layer 16 is a thin layer of very burnt, compacted sediment, observed across the majority (but not entire) excavation plan.

Below the shell midden (layer 10) and its associated basal hearth deposits (layers 11—16) is a very thick layer (layer 17) of reddish-brown (7.5 YR 4/3—4) sediments with an increase in rock inclusions compared to layers above. Layer 17 is generally homogenous with regards to grain size and sorting but does see a slight gradient from moderately sorted sandy silt at the top to a more gravelly, poorly sorted silty sand at its base. While small inclusions of charcoal occur sporadically throughout this layer, the ash observed in layers above is absent. The transition to layer 18 is marked by a distinct increase in sediment compaction, a redder colouration (7.5 YR 4—3/3) to the soil and the re-appearance of ash

lenses. Layer 18 contains a number of rocky inclusions like layer 17 but the matrix appears to be less gravelly, a slightly better sorted silty sand, than the layer above. The contact between layer 18 and the underlying, sterile sand is very uneven (Fig. 6).

The contents of layers 1—18, in addition to evidence indicating humans as the major agents of cave sediment accumulation in the region (Louys et al., 2017), strongly supports a cultural origin for these layers. However, they are underlain by a distinctive, culturally sterile, sand, suggestive of a very different sedimentation process. Thin section analysis was therefore conducted on a block sample recovered from this sand layer cross-cut in spit 68 of square B (Fig. 6). This analysis showed the deposit to be dominated by calcium carbonate grains, representing ~90—95% of the total composition of the sediment (Supplementary Information S4, Fig. S4.1). When viewed under cross polarized light (XPL), these grains show extinction banding indicative of a biological origin. These biological, carbonate grains are likely the product of the mechanical breakdown of marine shells and corals, and indeed larger identifiable shell and coral fragments were present and recovered for radiocarbon dating.

The remaining ~5—10% of the thin section is comprised of non-carbonate material, the majority of which are black, grey, and red lithic fragments (~5—8%). The internal composition of these lithic fragments shows a porphyritic texture of larger silt-sized phenocrysts (possibly feldspars) within a microcrystalline opaque groundmass, evidence that these are of volcanic origin. The final ~2—5% of grains are mainly heavy mineral (e.g., tourmaline) and feldspar grains of different varieties. After deposition, the carbonate rich sediment has been lightly cemented. Grain size is medium sand, moderately sorted, suggesting a high energy, near-shore environment, such as a beach. The complete lack of fine-grained silts and clays within the sediments further supports this hypothesis (Tucker, 2001). This basal, culturally sterile layer is therefore considered to represent a beach deposit, most likely lain down inside the cave at a time when it was still subject to at least occasional incursion by the sea.

3.1.2. Occupation phases at Makpan

Based on their associated dates (Table 1), each of the eighteen layers identified in the stratigraphy at Makpan (Figs. 5 and 6) was assigned to one of five major phases which were modelled accordingly in the Bayesian analysis. Double boundaries were inserted between each of the phases in the model to test for discontinuous sedimentation rates and possible hiatuses in the record.

Phase 1: the Late Pleistocene

Phase 1 is the period of initial occupation at Makpan with a median modelled start date of ca. 43,076 BP (49,192—39,073 BP; Fig. 7, Table S1). This phase recovered the oldest *in situ* date for the site of 40,241—38,453 cal BP (35,130 ± 414 ANU_51,417) and the earliest direct date for human activity at Makpan of 40,360—38,585 cal BP (35,232 ± 427 ANU_53,609). Phase 1 corresponds to stratigraphic layer 18 (spits 68—58), covering a period of ca. 28,000 years, and is distinct for its sparse marine fauna and generally sporadic low-density occupation.

Phase 2: the Terminal Pleistocene

Phase 2 represents the onset of dense occupation and rapid sedimentation at Makpan, with a median modelled start date of ca. 13,965 BP (15,103—13,427 BP; Fig. 7, Table S1). Corresponding to layer 17 (spits 57—37), this phase documents a significant increase in sedimentation rate and occupation density from phase 1 (over

1 m of deposit for a period of less than 2000 years), along with the first appearance of shell fishhook technology. A human tooth was also recovered from the base of this phase (Roberts et al., 2020), as well as a fragmented human ulna from the middle (spit 44) of phase 2.

Phase 3: the Pleistocene-Holocene Transition (a.k.a 'the midden')

Phase 3 refers to the substantial shell midden deposit preserved at Makpan, with a mean modelled start date of ca. 11,805 BP (12,021–11,411 BP; Fig. 7, Table S1). Spanning layers 16–10 (spits 36–21), this phase can be subdivided into an upper dense midden deposit (layer 10), underlain by a series of thinner layers comparatively less dense in shell but comprising numerous hearths, ash and burnt sediment layers (Fig. 6). Dating from phase 3 suggests sedimentation of this midden deposit and the hearths which preceded it was exceptionally rapid. In fact, the difference between the mean modelled end date (11,223 BP; Fig. 7, Table S1) and start date suggests a depositional period of just ~582 years. Furthermore, the 95.4% probability range for the end of this phase (11,733–10,889 BP; Fig. 7, Table S1) overlaps with the start range, indicating that phase 3 could have been deposited even more rapidly.

Phase 4: the Early-Middle Holocene

Phase 4 begins ca. 10,430 BP (11,063–9986 BP; Fig. 7, Table S1) and spans layers 9 to 5 (spits 20–9). A burial of a child dated to ca. 7.9 ka cal BP (ANU 56516) was recovered in the upper part of this phase (Table 1; Fig. 6), while a couple of fragmented human phalanges, unrelated to the child burial, were recovered from the base (spit 20). The transition between phase 3 and phase 4 sees a decline or cessation in occupation, but cultural material increases again over the ca. 3000-year period of phase 4.

Phase 5: the Neolithic-Historic

Phase 5 is the final phase of occupation at Makpan and pertains to the upper pottery-bearing layers, with a median modelled start date of ca. 3663 BP (5177 - 2398 BP; Fig. 7, Table S1). Comprising the top 4 layers (spits 8–1) of the deposit, this phase can be subdivided into an earlier Neolithic period (layers 4 & 3) and a final historic period (layers 2 & 1). The model predicts occupation at Makpan extending into the present, a prediction supported by evidence for continued sporadic cave use by local villagers observed during excavation.

3.1.3. Hiatuses in the record

Analysis of the predicted start and stop dates for the five key phases of occupation found no support for a discontinuity between the Late Pleistocene (P1) and Terminal Pleistocene (P2) phases, nor between phase 2 and the Pleistocene-Holocene Transition (P3). However, a minor hiatus between phase 3 and the Early-Middle Holocene (P4), and a significant gap in the record between phase 4 and the Neolithic/Historic (P5) phase was identified by our model (Fig. 8). As the mean age of each modelled boundary falls outside the 95.4% probability range of the other (Fig. 8A), and the 95.4% probability range of the difference model does not cross the 0 [zero] interval (Fig. 8B), there is a 95.4% probability of a discontinuity in the record between phases 3 and 4, and phases 4 and 5 (see also Supplementary Information S3). The P4–P5 hiatus in particular is substantial, ca. 3500 years between ca. 7284 to 3663 BP (Fig. 8; Table S1), supporting a scenario of either significant site abandonment or erosion at Makpan during this period. The disparate dates from the Late Pleistocene, phase 1 (Table 1) suggests there is

likely at least one additional hiatus in the Makpan record, however, the extremely compacted nature of this lower layer in addition to the significantly slower rates of sedimentation make it difficult to conduct more detailed chronological analyses at this stage.

3.2. Site formation at Makpan

3.2.1. Basal beach deposit

Today, the beach near Makpan is visually similar to the basal deposit in the cave, with a similar biologically-rich composition (see Supplementary Fig. S4.2). Biological (i.e. shells and corals) origins for the majority of beach sand composition, mixed with some volcanically-derived grains is a common occurrence on beaches throughout the region (Koesoemadinata and Noya, 1989; Janßen et al., 2017), the result of rich reef environments surrounding islands of volcanic origin, many of which still support active volcanoes (see Koesoemadinata and Noya, 1989). This combination of beach-forming components has existed on Alor since at least the Pliocene (as evidenced by the different geological formations preserved on the island today; Koesoemadinata and Noya, 1989), making it highly probable that similar beach deposits have been forming since this time.

Alternative, non-marine origins for this basal deposit at Makpan can be discounted based on the composition of the sediment. A high ratio of biological carbonate grains of marine origin would be highly unlikely to accumulate in freshwater (e.g. river, stream). Similarly, the large grain size (medium sand), makes windblown sedimentation (which very rarely accumulates grains larger than fine sand; Vandenberghe, 2013) of this deposit unlikely (Tucker, 2001). Finally, there remains some possibility that this deposit was the result of a storm surge or tsunami, however Makpan has stood at least 15 m above sea level ever since ca. 48 ka (Fig. 9), making it unlikely the deposit is the result of storm surge (Astiduari et al., 2018; Nott et al., 2014) following the sites rise above the level of beach formation. As for a tsunami origin for the deposit, the lack of sedimentary characteristics, such as rip-up clasts, mud caps, and strong evidence that the deposit is at least >25 cm thick, all support standard beach depositional processes for this deposit (Phantuwongraj and Choowong, 2012; Morton et al., 2007; Tucker, 2001).

3.2.2. Sedimentation rates and stratigraphic integrity

Throughout the cultural layers of the Makpan record the rates of sedimentation change substantially. When we consider that humans are the major agent of cave sediment accumulation in the region (Louys et al., 2017), these rates can act as a proxy for general changes in occupation intensity at the site over time. Table 2 shows two different calculations for average sedimentation rate for each of the five phases at Makpan. The midden (P3) is clearly highlighted as the phase during which the most rapid sedimentation occurred. Table 2 calculates a significantly lower rate of sedimentation for phase 1 than any period of occupation thereafter.

The exceptionally slow sedimentation rate during phase 1, resulting in an average of less than 2 cm of sediment accumulating every 1000 years (Table 2), likely contributed to some of the inversions in dates seen in this phase. Such low rates of sedimentation increase the risk of vertical movement of larger fragments (e.g. shells) within the deposit which, compounded by the compacting effect of the dense and rapidly deposited sediments above, have resulted in a deposit within which ~25 ka and ~40 ka materials cannot be readily distinguished at this time. Future excavations to recover a more extensive record across a broader expanse of the cave may uncover better preserved sections of the phase 1 deposit, clarifying its chronology.

The next phase sees the second-most rapid sedimentation rate
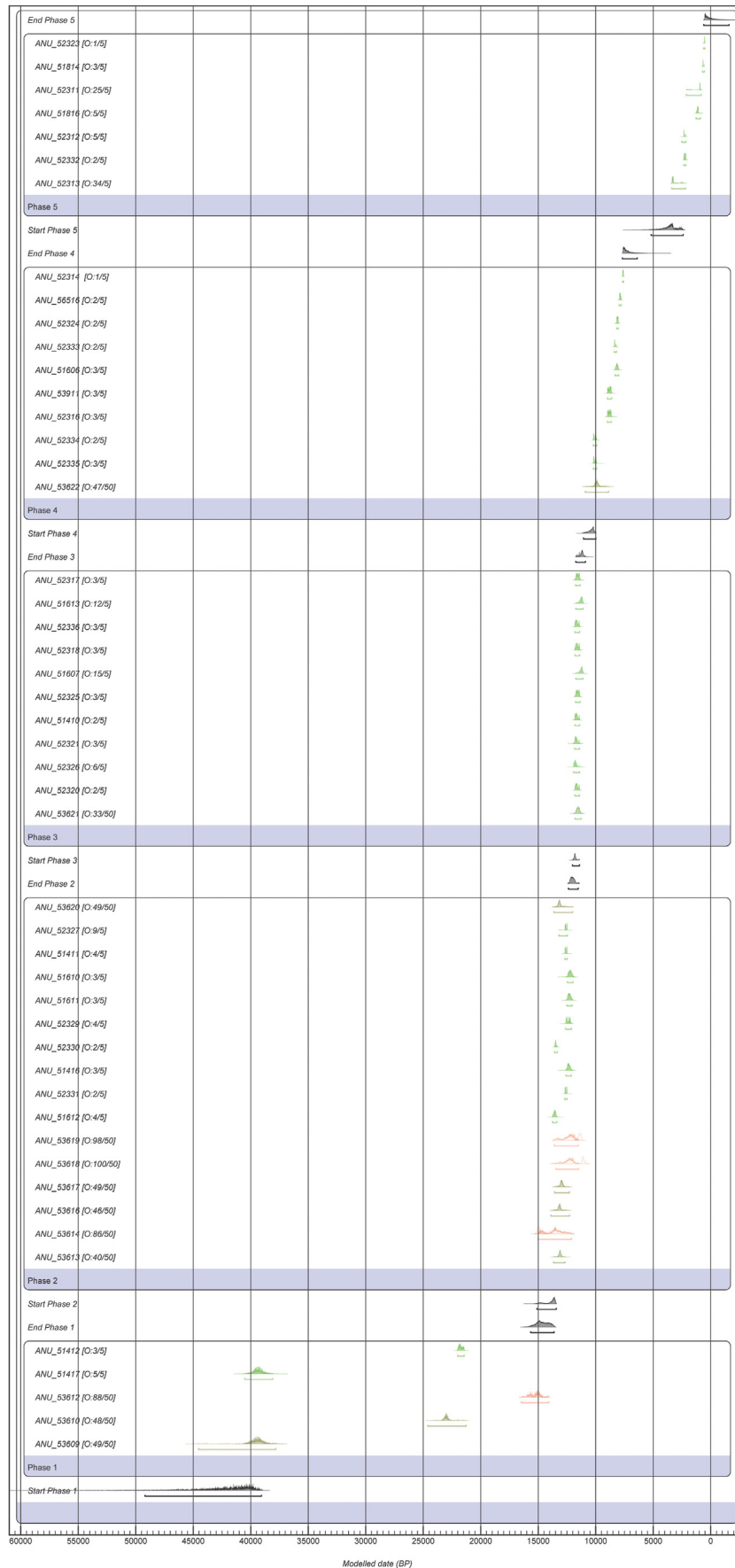
across the Makpan deposit (Table 2) with no inversions recorded in the *in situ* dates (Table S1) and only three of seven (non-*in situ*) dates identified as significant outliers (>50% probability) in the model (Fig. 7). Above this, all *in situ* dates fit the model with less than 5% outlier probability, while none of the non-*in situ* are identified as significant outliers (<50% probability; Fig. 7). In addition to congruity in dates across these phases at Makpan, the high number of well-preserved ash lenses at the base of phase 3, and throughout phases 3, 4, and 5, further supports the stratigraphic integrity of the Makpan assemblage. The intact rock-floor feature from layer 4 at the base of phase 5, and a conjoined lithic artefact recovered from spit 34 in the lower portion of phase 3, reinforce the reliability in associations between cultural materials and stratigraphic context for the upper 4 phases at Makpan.

3.3. Establishing the uplift rate for Makpan

Samples from the oriented sediment block of culturally sterile beach deposit returned a radiocarbon age close to the background limit for carbonates: 48,954 ± 1033 BP (Wk 49,506). An attempt to calibrate the date in OxCal v. 4.4 (Ramsey, 2009a) suggests it is older than 49 ka (at 95.4% probability), however, this is right at the edge of the calibration curve and a portion of the radiocarbon determination falls outside the range of the curve. When only the 1σ (68% range) probability is considered OxCal suggests an age of 54,047–49,825 cal BP.

For the period between 54 and 49 ka the sea level around Alor Island is predicted to have fluctuated between ~70 and 53 m below present levels (Lambeck and Chappell, 2001). The highest sea level (−53 m) during this time occurred at ca. 52 ka and is the most likely estimate for the age of the sandy carbonate deposit. An uplift rate estimate for the Makpan region of 1.67 m/ka was obtained from the following formula based on Cox (2009):

$$SU = \frac{(CE - SL_{age})}{age}$$

where: SU = Surface Uplift, CE = Current Elevation of the sample (in meters), SL_{age} = Predicted Sea Level for the given age (in meters relative to present), and *age* = the age of the sample (in thousands of years).

An uplift rate of 1.67 m/ka is notably faster than that observed by Hantoro et al. (1994) on Alor's north-west coast, but the estimate of 1.0−1.2 m/ka (Hantoro et al., 1994) would push back beach formation prior to 70 ka (Fig. 9), which is at odds with our age estimate for the beach deposit. Even if the maximum Hantoro et al. (1994) uplift rate of 1.2 m/ka were used, this would require a storm surge to have deposited these beach sediments at a height of over 20 m above the sea level at the time (Fig. 9), an extremely unlikely scenario considering the world record for largest storm surge is just ~13 m (Nott et al., 2014). When we consider the often markedly different uplift rates obtained from neighbouring regions of nearby Timor (Cox, 2009), and the high tectonic activity of the region in general (Major et al., 2013), it is not implausible to have a difference of ~0.5 m/ka in uplift rates between the northern and southern coasts of Alor. As Hantoro et al. (1994) point out, their uplift estimate for Alor is twice as fast as those calculated for nearby Atauro and Sumba islands, while being slower than rates more recently estimated for Rote (Roosmawati and Harris, 2009) and Timor (Cox,

2009). Furthermore, uplift rates are known to vary over time (Shen et al., 2018), particularly in such a tectonically active region (Pedoja et al., 2014).

Of course, any rate based on just a single date can only provide us with a very simplified uplift estimate, with substantial survey work required all along the Alor coast to further resolve patterns of uplift on the island across time and space. Such efforts are outside the scope of our study. Nevertheless, and given the Hantoro et al. (1994) estimate is a poor fit with the geological records recovered from Makpan, we suggest 1.67 m/ka to be the best-fit currently available model of long-term average uplift for the coast around Makpan, and possibly the greater southwest corner of Alor. Hereafter all mentions of sea level refers to adjusted sea level (i.e. sea level adjusted for 1.67 m/ka uplift; see Fig. 9) unless otherwise stated.

3.4. Makpan cultural materials

3.4.1. Stone artefacts

Eight grindstones and anvils, 25 cobble manuports, and 4542 flaked stone artefacts were recovered from square B (Fig. 10, Table 3; Table S2). Cobbles occur sporadically in all phases, while grinding stones and anvils occur from phase 2 (spit 44) and above. The knapped artefacts include flakes struck from used cobbles, including one shown in Fig. 11D that had ochre residue deposited prior to it being removed from the cobble. Cores are rare throughout the assemblage, but represented types include discoidal, multi-platform, and single-platform, and, in the case of obsidian artefacts, large numbers of bipolar cores. While both cores and flakes were recovered from phase 1, artefacts showing retouch were only recovered from phase 2. Four lithic materials were flaked at Makpan: obsidian, chert, chalcedony, and basalt, the latter including some very fine-grained varieties (Fig. 11; Table 3). Marine shell flakes were also identified. All lithic raw materials are potentially locally available on Alor, with the basalts in particular occurring close to the site (Shipton et al. forthcoming).

In the first phase of occupation, obsidian, chert, and basalts are all well-represented, while there is a single chalcedony artefact. In the second phase there is more chert, less basalt (both coarse and fine) and shell flakes appear. In the third phase obsidian use increases, there is more chalcedony, and little coarse basalt. Obsidian constitutes two-thirds of the flaked material in phase 4, with corresponding reductions in the use of all other materials. Phase 5 sees a relative reduction in obsidian and an increase in chert. A chisquare test indicated that the differences in the four main material types (chert, obsidian, and fine and coarse basalt) across the phases are highly significant (χ = 293.379, p < 0.00001). These changes in material composition reflect changing provisioning strategies, likely in response to the changing landscape around Makpan.

3.4.2. Items of maritime technology and personal ornamentation

Some 794 pieces of fishing technology and items of personal ornamentation made on marine shell and coral have thus far been recovered from square B. This extensive assemblage includes artefacts representing all stages of manufacture for both jabbing and rotating fishhooks made on *Rochia nilotica* and *Turbo* sp. (Fig. 12A−C & E), along with possible lures (Fig. 12D), a probable coral sinker, a fragment of finger coral with evidence for use and

---

Fig. 7. Bayesian date model for the Makpan archaeological sequence. Calibrations were made using OxCal v4.4 (Ramsey, 2017, 2009a), and IntCal20 (Reimer et al., 2020) for charcoal or Marine20 for marine shell (Heaton et al., 2020). Green indicates dates which fit well within the model while red indicates significant (>50% probability) outliers. Modelled start and end distributions for the different layers are in grey. The brackets beneath the distributions represent the 95.4% probability range. Prior and posterior outlier probabilities are given in brackets following the sample name in the form [O: posterior/prior]. (For interpretation of the references to colour in this figure legend, the reader is referred to the Web version of this article.)
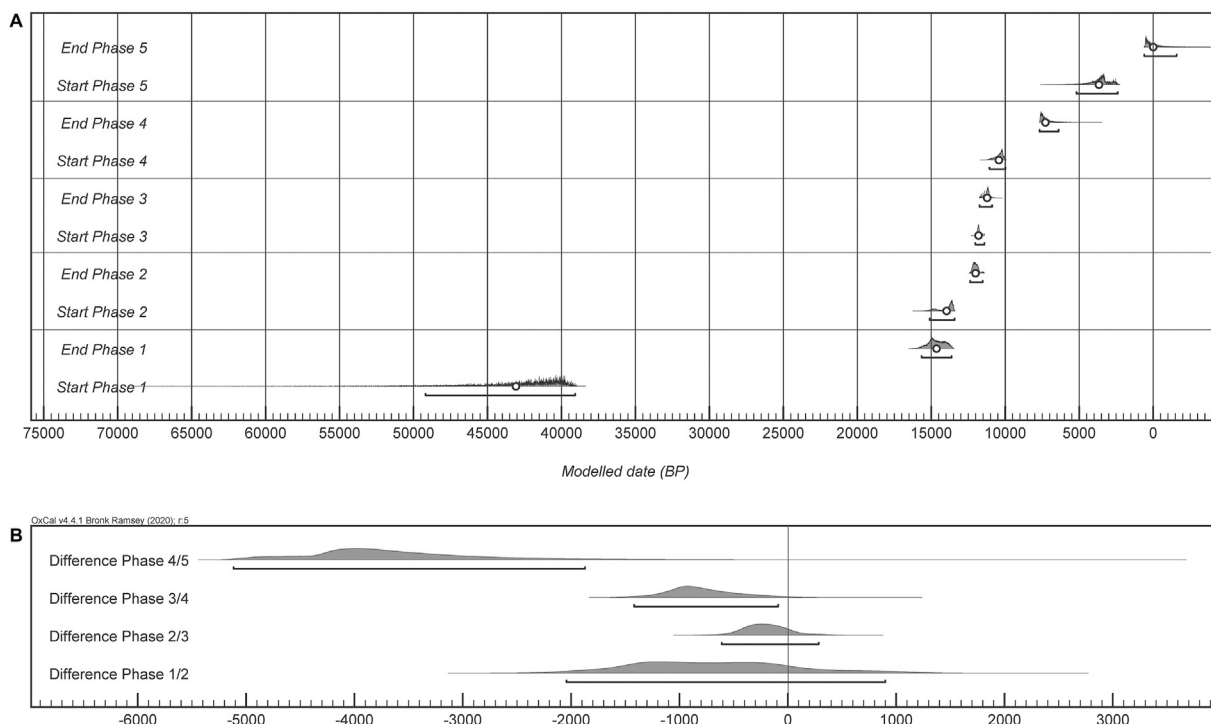
Fig. 8. Modelled dates for the different occupation phases at Makpan (A) and the results of the difference analysis between them (B), (see also Supplementary Info S3).
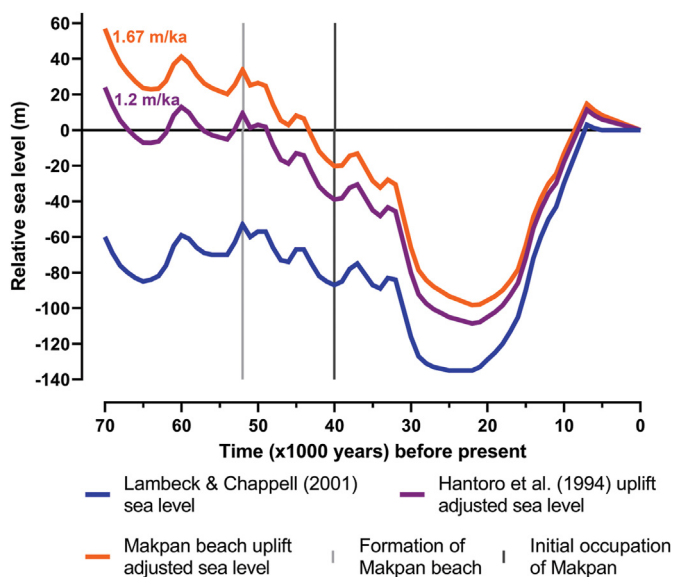

Fig. 9. Sea levels (relative to present) near Makpan adjusted for uplift. Blue shows the original sea level model of Lambeck and Chappell (2001), purple shows the sea level adjusted for a 1.2 m/ka uplift rate, and orange is adjusted for a 1.67 m/ka uplift rate. Vertical lines indicate final beach deposition at Makpan (grey) and initial occupation (black). (For interpretation of the references to colour in this figure legend, the reader is referred to the Web version of this article.)

Table 2
Average sedimentation rates for each phase of occupation at Makpan calculated by both volume and depth.

Phase	Time[a] (yrs)	Sediment[b] (kg)	Rate[c] kg/ka	Depth[d] (cm)	Rate[c] cm/ka
P5	3663	561.79	153.37	40	10.92
P4	3146	619.88	197.04	55	17.48
P3	582	741.20	1273.53	80	137.46
P2	1959	1239.45	632.70	105	53.60
P1	28,431	672.03	23.64	50	1.76

[a] Time lapsed between the mean modelled start and end dates for the phase (see Table S1).
[b] Total excavated sediment weight for the phase (see Table S2).
[c] Average sedimentation rate for the phase (to 2 d. p.).
[d] Average depth of the phase (see Figs. 5 and 6).

both types of shell artefacts (fishhooks and beads), the densest concentrations of both intact (or near intact) and fragmentary items occur in phase 2. Five artefacts made on either *Rochia* or *Nautilus* appear morphologically consistent with lures. Aside from the fishhooks and lures, two coral items were recovered. A probable net or line sinker with holes drilled for fibre attachments (Fig. 12F), and a likely drill/file made from a finger coral (Fig. 12G). A similar finger coral artefact with wear resulting from use as a tool, perhaps for shell fishhook production (O'Connor et al., 2019), was recovered from Here Sorot Entapa on Kisar (O'Connor et al., 2019). Ethnographic records from Northern Queensland, Australia, document the use of finger coral as "drills" and "files" for the manufacture of shell fishhooks (Roth, 1904:33), supporting a similar purpose at Makpan.

Shell flakes presumed to be detached from thick clam shells or large *Turbo* opercula were also recovered at Makpan, suggesting additional shell technologies unrelated to fishhook manufacture. These shell flakes are densest during phase 3 (Table 3), coinciding with the same period of increased manufacture of the other shell artefacts, and increased occupation more generally.

various items of shell ornamentation.

Shell technology is present from the initial phase of occupation at Makpan (Table 4), with single disc and two-holed oval-shaped beads made on *Nautilus pompilius* occurring in spit 63 (P1) (Fig. 12H). Shell fishhooks first appear in the earliest levels of phase 2 (Table 4; Langley et al., 2020), coinciding with intensification of site use and an increase in exploitation of marine resources. For
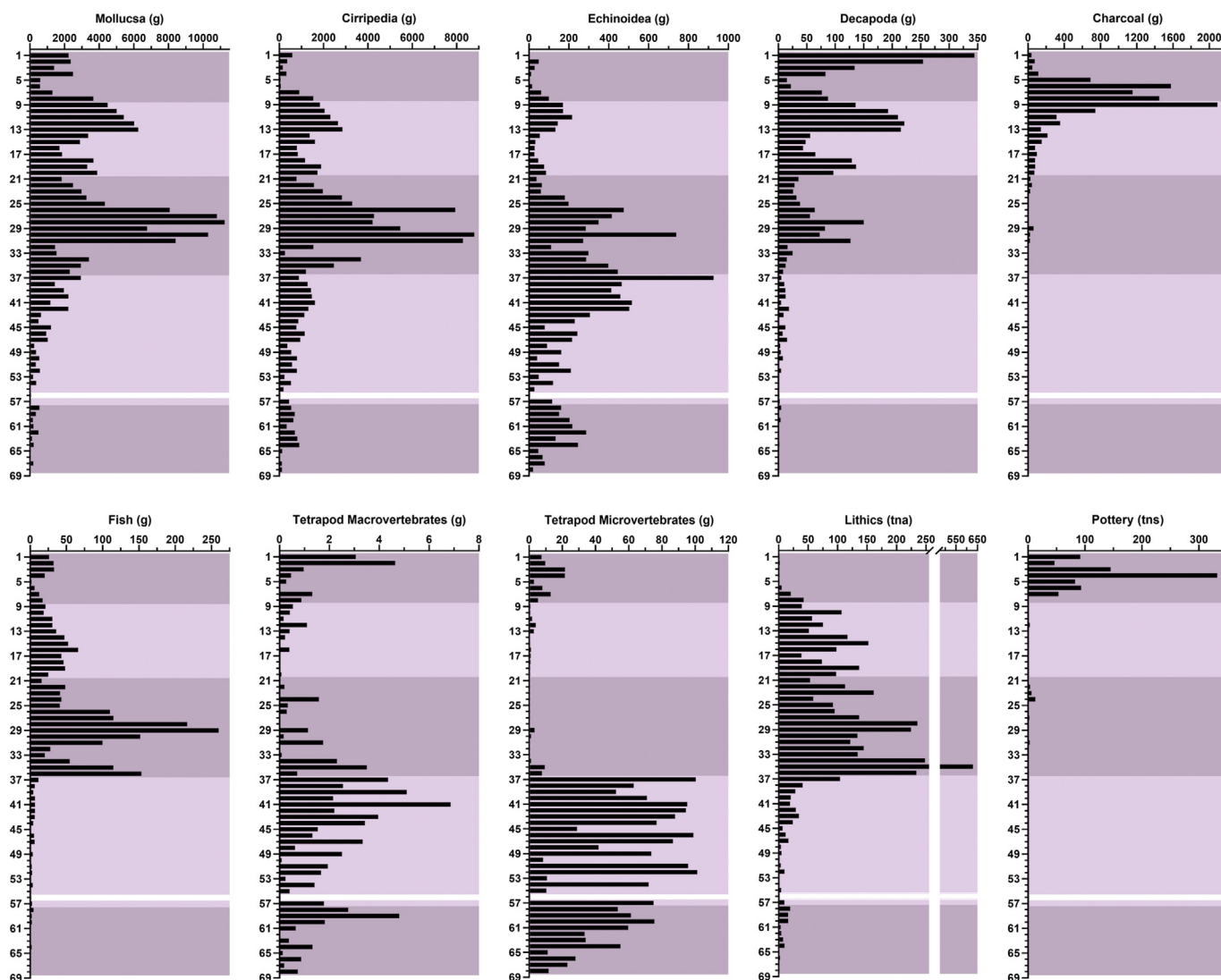
Fig. 10. Cultural material recovered from the Makpan excavation. Bars indicate amount of material per spit, adjusted for total spit volume (see Table S2). Shading corresponds to the 5 identified phases.

Table 3
Breakdown of flaked artefacts by material and phase for Makpan square B.

Phase	Obsidian	Chert	Chalcedony	Glossy Green[a]	Coarse Basalt	Fine Basalt	Shell	Total
P5	79 (54%)	42 (28%)	2 (1%)	0	11 (8%)	13 (9%)	0	147 (100%)
P4	715 (67%)	161 (15%)	24 (2%)	1 (<1%)	64 (6%)	105 (10%)	2 (<1%)	1072 (100%)
P3	1219 (44%)	606 (22%)	130 (5%)	34 (1%)	206 (7%)	576 (21%)	13 (<1%)	2784 (100%)
P2	156 (35%)	164 (36%)	6 (1%)	2 (<1%)	66 (15%)	55 (12%)	2 (<1%)	451 (100%)
P1	28 (32%)	18 (20%)	1 (1%)	0	19 (22%)	22 (25%)	0	88 (100%)
Total	2194	989	163	37	366	741	17	4542

[a] Glossy green refers to a material with these particular physical characteristics that is likely a chert variety.

3.4.3. Pottery

A total of 1169 sherds of low-fired, earthenware pottery, weighing a little over 1040 g was recovered from square B (Table 5). The vast majority of these were fragments of vessel bodies, but 20 rim sherds were identified. Twenty-four sherds preserve decoration and a large proportion of sherds have evidence of surface treatments including red, black, and brown slips, and combinations of these applied surface colours (see Supplementary Information S5).

While some sherds were recovered down to spit 31, based on the fact that there is a hiatus between the Neolithic (P5) and the early to mid-Holocene (P4), the small size and low numbers of sherds below spit 7 (18 sherds of a total of 1169; Table 5), and the loose nature of the underlying midden deposit, we consider it highly likely that the sherds below the Neolithic phase 5 are intrusive. Vertical displacement of pottery is a commonly noted occurrence in cave deposits (see Spriggs, 1996:43−44; O'Connor et al., 2011a).

In addition, a small number of baked clay fragments were recovered from spits 17, 22, 23, 24 and 31 (Table 5). Most of these
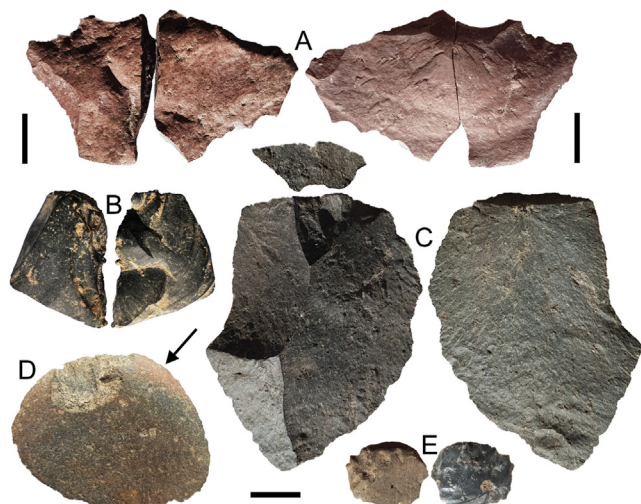
Fig. 11. Flaked lithics from the Makpan excavation. A) conjoined siret break on a chert flake from spit B34; B) fine basalt flake from spit B48; C) basalt flake from spit B35; D) flake from basalt cobble with ochre (denoted by the arrow) on the dorsal surface; E) fine basalt flake from spit B32.

fragments are relatively small, measuring less than 15 × 15 mm. However, the occurrence of baked clay pieces in pre-pottery contexts may represent the use of clay hearth liners, as recently reported from Sulawesi dating from ca. 9900-8800 cal BP (Bulbeck et al., 2019).

3.4.4. Vertebrate fauna

The Makpan excavation recovered a dense vertebrate assemblage with fish dominating the anthropogenic fauna. A notable proportion of these fish remains show evidence for burning, preserving a colouration range from partial blackening to fully white (Samper Carro et al., 2016b). Detailed taphonomic analysis of this assemblage will be published elsewhere. The fish assemblage includes over 2 kg of fish bone (Table S2), tens of thousands of specimens, predominantly from small to medium-sized inshore/ reef fish, including Balistidae (triggerfishes), Labridae (wrasses), and Serranidae (sea basses and groupers). These three taxon groups are dominant in the Makpan assemblage; however, they represent only a small portion of the greater marine biodiversity in the region (e.g. analysis of fish bone at Here Sorot Entapa, Kisar, identified 27 different fish families; O'Connor et al., 2019). Some specimens have

been identified as Scombridae (e.g. mackerel, bonito, tuna), which includes the pelagic tuna, suggesting these fish were also occasionally caught and consumed at Makpan. Fishing strategies for these taxa may have involved maritime crafts, but could have been just as easily caught near-shore by angling, netting, or spearing (Ono, 2010). Other families identified in the Makpan fish assemblage thus far include Holocentridae (squirrel- and soldierfish), Scaridae (parrotfish), Lethrinidae (emperor fishes), Acanthuridae (surgeonfishes, tangs, and unicornfishes), Kyphosidae (sea chubs), and Diodontidae (porcupinefishes). In addition to these ray-finned fishes, remains of cartilaginous fish (Chondrichthyes; i.e. sharks/ rays) were also recovered from Makpan in small amounts.

Of the tetrapod vertebrates, the vast majority are microvertebrates, with rodents (including the endemic giant rat previously described in Louys et al. (2018)) predominating. As owls are known to have occupied the cave both in the past (Louys et al., 2018) and present day, the likelihood is that the majority (if not all) of this assemblage accumulated from owl predation and not the result of human subsistence. The remains of larger species (i.e. >180 g) are less likely to be deposited as the result of owl predation and are here assigned to human subsistence; however research as to the precise agency of the giant rats is ongoing. The macrovertebrates were recovered in significantly smaller amounts (~100 g total; Table S2), with a scattered distribution throughout the assemblage (Fig. 10), suggestive of more opportunistic hunting rather than a dedicated subsistence strategy. Macrovertebrates (e.g. turtles, adult giant rats) were, however, recovered from the beginning of phase 1, indicating a continuous, albeit minor, component of the Makpan diet. A slight increase in macrovertebrates in the upper part of the final occupation (P5) likely reflects the consumption and discard of occasional domestic animals.

The bulk (by weight) of the tetrapod microvertebrate remains were recovered from the Late and terminal Pleistocene (P1 & P2; Fig. 10; Table S2). This result is in stark contrast to the fish remains which increase notably in the initial Holocene sequence (P3). While fish remains were recovered from phase 1 and 2, there is a very clear increase in abundance from the very beginning of phase 3 (Fig. 10). The increase in fishing at this stage appears to coincide with a significant increase in shellfishing, and the formation of the dense midden deposit.

Based on comparisons with the rest of the cultural assemblage (Fig. 10) and in light of the likely owl roost contribution, we consider the fish assemblage to be a 'true' reflection of occupation intensity at Makpan. While there are rare and occasional incidences
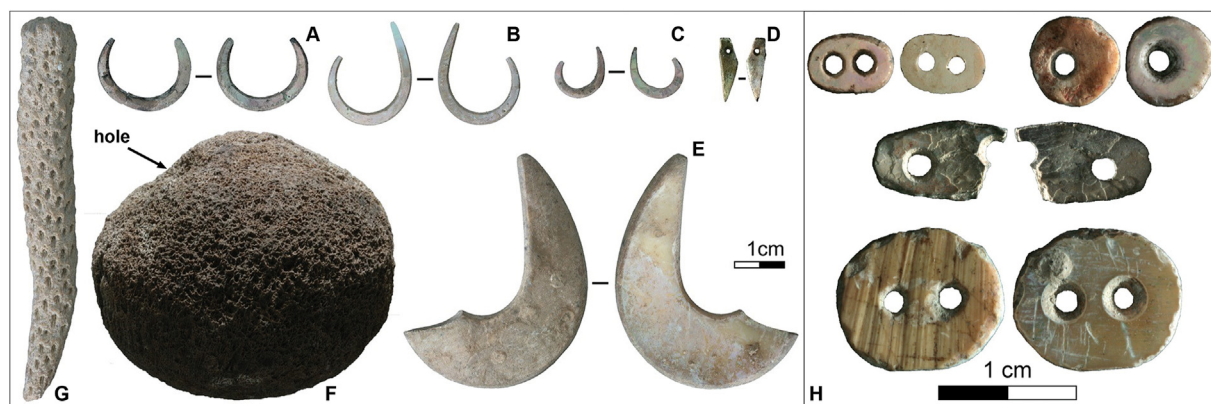
Fig. 12. Marine shell and coral fishing (at left) and ornamentation (at right) technologies from Makpan. (A) rotating fishhook, spit 23; (B) jabbing fishhook, square B north wall; (C) small jabbing fishhook, spit 29; (D) possible shell lure, spit 18; (E) large jabbing fishhook, spit 48; (F) perforated coral sinker, spit 30; (G) finger-coral tool, spit 29; (H) selection of single-holed disc beads and two-holed oval beads made on *Nautilus pompilius* from square B.

Table 4
Numbers of shell fishing artefacts recovered from Makpan, square B.

Phase	Spit[a]	Circular Hook		Jabbing Hook		Lure	Fragment/Blank
		Rough-out & Preform	Finished	Rough-out & Preform	Finished		
P5	5						1
P4	11						1
	15						1
	17						2
	18					2	
P3	20	1					1
	23		1	1			1
	24			1			2
	25	1					1
	26	3		2			18
	27	2		5		1	10
	28	2			1	1	26
	29			2	2		12
	30	1		3	2		5
	31			1	2		44
	32			1			5
	33	1			1		1
	34			1			1
	35			2			10
	36		1	3			11
P2	37						2
	38			1			8
	39					1	3
	40			1			1
	42	1					
	44				1		
	47				1		
	48				1		
	49						
	54	1					
	Total	13	2	24	11	5	167

[a] Note: Only spits from which artefacts were recovered are listed here, missing spits indicate that no artefacts were recovered from those spits.

Table 5
Pottery sherds recovered from Makpan square B.

Phase	Spit	#	Weight (g)	Body	Rim	N/S/C/B[a]	Decorated	Baked Clay
P5	1	149	182.09	149			1	
	2	76	56.92	75	1		2	
	3	120	101.86	117	3		4	
	4	515	370.70	503	11	1	14	
	5	127	130.47	124	2	1	3	
	6	91	114.04	88	3			
	7	73	55.06	73				
	8	3	1.67	3				
P4	9	1	2.01	1				
	10	2	4.29	2				
	11							
	12	4	5.12	4				
	13							
	14							
	15	1	0.65	1				
	16							
	17	3	0.67	1		1		1
	18							
	19							
	20							
P3	21							
	22	5	1.09					5
	23	8	7.32					8
	24	11	2.71					11
	25							
	26							
	27	3	9.87	3				
	28							
	29	1	1.01	1				
	30							
	31	3	0.88	1				2
Total		**1196**	**1048.43**	**1146**	**20**	**3**	**24**	**27**

[a] Neck/shoulder/carination/base.

of owl-deposited fish remains (Taylor, 2004; Broughton et al., 2006; Romano et al., 2020), the overwhelming abundance, substantial size range, and presence of both near and off shore species makes it highly unlikely that the majority of this fish assemblage is the result of owl activities. The negative association between the microvertebrate (common owl prey) assemblage and fish (uncommon owl prey) assemblage further emphasises these associations. The presence of an owl at the site currently, while it is still used sporadically by local people, indicates that owls and people may have co-habited at Makpan in the past. Although, during periods of intense and permanent use of the cave by people, Makpan likely became a significantly less attractive roost location for the local owls. Thus, the tetrapod microvertebrate assemblage is likely a good indicator of periods of low intensity and/or sporadic/seasonal human occupation at Makpan, while the fish assemblage indicates the reverse.

3.4.5. Molluscan invertebrate fauna

Over 173 kg of aquatic mollusc (i.e. shell) remains were recovered from the square B excavation (Table S2). Shell abundance begins to increase noticeably during phase 3, creating the Pleistocene/Holocene Midden deposit (P3), with the greatest peak in shell consumption occurring in the middle of the phase. The beginning of phase 4 sees a decline in shell abundance, but this dip is followed by a secondary peak in shell subsistence toward the end of this phase (Fig. 10). In addition to shell flakes and artefacts, further evidence for anthropogenic modification to portions of the shell assemblage is the occasional presence of burnt and partially burnt shells through the assemblage, with the highest density of such pieces in phase 2 and 3.

We identified 30 species of Gastropoda, seven species of Bivalvia, a species of Cephalopoda, and at least one species of Polyplacophora. The following 11 gastropod families have been identified: Conidae (*Conus*), Cypraeidae (*Cypraea, Naria, Mauritia*), Haliotidae (*Haliotis*), Littorinidae (*Tectarius, Echinolittorina*), Muricidae (*Drupa, Thais, Drupella, Purpura, Tenguella*), Nacellidae (*Cellana*), Neritidae (*Nerita*), Patellidae (*Scutellastra*), Tegulidae (*Rochia*), Trochidae (*Enida, Infundibulum*), and Turbinidae (*Turbo*). Four bivalve families have been identified: Cardiidae (*Hippopus, Tridacna*), Mytilidae (*Perna*), Osteridae (*Saccostrea*), and Psammobiidae (*Asaphis*). The single family of Cephalopoda identified is Nautilidae (*Nautilus*). Within Polyplacophora numerous specimens belonging to the family Chitonidae were recognised, however their genus and species-level identifications remain unresolved. This range of shells is found throughout the sequence and derives from a variety of marine habitats including sandy beach, rocky foreshore, and coral reefs. Rocky platform taxa, however, and in particular limpet species (*Scutellastra* spp., and *Cellana* spp.) as well as *Nerita* spp., *Strombus* spp., *Rochia* spp., *Turbo* sp., *Haliotis* sp., and *Chiton* spp., are by far the most abundant.

3.4.6. Non-molluscan invertebrate fauna

A total of 109.4 kg of Cirripedian (Barnacles) remains were recovered from Makpan square B (Table S2). The trends in barnacle subsistence throughout the sequence strongly correspond with the marine mollusc shell assemblage (section 3.2.5; Fig. 10). This finding is unsurprising as, while taxonomically a crustacea, barnacles closely resemble the physical and ecological properties of marine mollusc shells (i.e. a hard external shell containing a fleshy body that lives a sessile lifestyle in rocky shore environments) and are found in the intertidal zone, so were probably collected by Makpans occupants while foraging for marine molluscs. The only slight difference in abundance trends between barnacles and marine Mollusca occurs in the final phase of occupation (P5) where we see a significant decline in barnacles while molluscs are comparatively more abundant.

Approximately 4 kg of Decapoda (crab and lobster) remains were recovered from the square B sequence (Table S2). Most of these remains were recovered from the upper portion of the deposit with abundance increasing notably in the midden phase (P3) and continuing into phases 4 and 5 (Fig. 10). Interestingly, the greatest abundance of crab and lobster remains was recovered from the top 10 cm of the deposit. While there are no documented cases of owl-deposited marine shell, barnacle, or sea urchin assemblages, owls have occasionally been recorded preying on crustaceans (Taylor, 2004; Obuch and Benda, 2009), including at a modern owl roost site in a sea cave on Alor's north-west coast (S.K. & J.L. pers. obs.). However, the high amount of decapod remains in the Makpan assemblage, lack of association with the microvertebrate (common owl prey) assemblage, and an absence of these invertebrates recorded in the known owl roost deposit excavated deeper in the cave (see Louys et al., 2018), suggests that the majority of the Makpan decapod assemblage was deposited due to human activity rather than that of owls.

Abundant (~14 kg) Echinoidea (sea urchin) remains were also excavated in square B (Table S2). Curiously, in contrast to fish, crab, barnacle, and shell, sea urchin consumption appears to have been especially prevalent during the Late and terminal Pleistocene (P1 & P2) occupation of the site (Fig. 10). At least six species of sea urchin were exploited, belonging to the four families of Diadematidae (genus unidentified), Echinometridae (*Colobocentrotus, Echinometra, Heterocentrotus*), Temnopleuridae (*Mespilia*), and Toxopneustidae (*Tripneustes*). The majority of these species originate from coral reef environments; however, rocky platform, sandy beach, and deep-sea species are also present. Within the assemblage, the coral reef and deep-sea species appear to be the most abundant. All species grow edible gonads (the only part of the animal consumed by humans) and require minimal processing efforts to extract and consume (Lawrence, 2007), leading to the application of the term "prehistoric fast food" (Burroughs, 2005; Kaharudin, 2020). While modern and historic records suggest urchins are commonly eaten raw (Lawrence, 2007; Kaharudin, 2020), some of the specimens in the Makpan assemblage do show evidence for burning, particularly from the hearth-rich layers at the base of phase 3.

4. Discussion

Extensive radiocarbon dating has demonstrated Makpan to be the oldest known site for human occupation on Alor Island with a date of ca. 40 ka cal BP from the basal layer of the deposit. Prior to the excavation of Makpan, the earliest evidence for occupation on Alor was from the rockshelter Tron Bon Lei to the east of Makpan, with a near basal age of ca. 21 ka cal BP (Samper Carro et al., 2016a, 2017; O'Connor et al., 2017b). The dates for initial occupation of Makpan demonstrate that colonisation of the island occurred much earlier than this. With a modelled start date for initial occupation at Makpan of ca. 43,076 BP, Alor island was probably occupied as early as Flores and Timor. The modelled age estimate of 49.19–39.07 ka BP (95.4% probability) for the initial occupation of Makpan overlaps all three oldest date ranges from the neighbouring sites of Laili (44.7–43.4 ka cal BP; Hawkins et al., 2017) and Asitau Kuru (46.5–43.1 ka cal BP; Shipton et al., 2019) on Timor-Leste, and Liang Bua on Flores (47.66–44.13 ka cal BP; Sutikna et al., 2018). While the sample with the oldest *in situ* date (ANU 51417) was obtained near the base of the cultural deposit, the compacted nature of this layer and the extensive area of living surface left unexcavated at the site, supports the possibility that earlier evidence for occupation at Makpan remains to be found. The Makpan record is therefore supportive of Alor island's involvement in a later stepping-stone

migration along the southern route from Sunda to Sahul (Fig. 1).

Following beach deposition ca. 52 ka into the cave entrance, a combination of lowering sea levels and tectonic uplift raised Makpan permanently above the level of marine incursion and presumably rendered it accessible for human occupation. Allowing for some leeway in our temporal predictions, this circumstance leaves a gap of ca. 10 ka between the time when Makpan was available for occupation and the time when the recovered archaeological record began to accumulate. The uneven contact between the lowest layers of cultural sediment and upper level of the beach deposit (Fig. 7; Fig. S4.2A) is indicative of an unconformity in this portion of the site's stratigraphy, suggesting that the culturally sterile and/or initial archaeological deposits may have been eroded (possibly by occasional high energy marine events following uplift above sea level but before exceeding heights of >15 m after ~48 ka), prior to the deposition of the lowest cultural layer recorded here. Freshwater flooding through the cave prior to ca. 41 ka could conceivably also have eroded some of the underlying deposit; however, if this was the case, then such action ceased after this time, with no evidence for water flowing through the site (e.g. carbonate precipitates, water-rolled materials) recovered from the Makpan cultural sequence (layers 1−18).

Between ca. 52 ka and ca. 40 ka sea level dropped by ~54 m and Makpan's position relative to the coastline changed, becoming more elevated and ~770 m distant (Fig. 4). Lowered sea levels resulted in the joining of Pantar island to the small island of Pura, significantly reducing the crossing distance between the two major islands of Pantar and Alor. In addition, the westwardly extending coastline of Alor's southwest coast as it emerged with lowered sea levels, further shrunk the crossing distance. The narrowing of this crossing may have provided further encouragement for the early movement of human groups from the west, precipitating arrival onto Alor.

Following initial occupation at Makpan, continued falls in sea levels owing to the onset of the Last Glacial phase resulted in the closing of the Pantar Strait by ca. 35 ka; specifically, the emergence of the land-bridge connecting the southwest coast of Alor to the island of Pura (and by extension Pantar). Closing the Pantar Strait would have blocked the strong ocean currents that flow through the channel when open. While these currents bring with them a diverse abundance of ocean resources (Ayers et al., 2014), the formation of a large, protected bay immediately adjacent to Makpan may have created favourable conditions for the growth of shallow water marine resources, facilitating their easy collection by people. As with sites on several other islands registering early occupation in Wallacea, such as Liang Sarru in the Talauds and Asitau Kuru in Timor-Leste, the record of site use at Makpan immediately following human arrival is sparse and episodic.

The marked increase in site occupation associated with phase 2 begins as rising sea levels bring Makpan back to a similar distance from the coast as it was at the time of initial occupation, while maintaining the landbridge between Alor and Pantar (Figs. 4 and 9). Isotopic analysis of a human tooth recovered from phase 2 suggests that terrestrial resources made up a significant proportion of the diet at Makpan during this time (Roberts et al., 2020). As our archaeological assemblage recovered very little evidence for terrestrial resource collection, this isotopic signature likely reflects consumption of plant materials which are unlikely to be preserved. Perhaps the increased distance to the coast during the LGM, in addition to general coastline instability across this period, encouraged Makpan's early inhabitants to supplement their marine, protein-rich diet with terrestrially sourced carbohydrates, leading to a heavy reliance on these resources by the beginning of phase 2 (Roberts et al., 2020). Post-LGM sea level rise reduced Makpan's distance from the coast to <1 km, enabling the recorded increase in

marine resource exploitation. This increase in the accessibility of protein in the diet of Makpan's inhabitants possibly enabled the increase in occupation intensity we see during phase 2.

A closer look at the marine invertebrate assemblage from Makpan supports not only increased occupation at Makpan during phases 2 and 3 but also a further increase in a diversity of ecological zone exploitation. Sea urchins in particular show a general trend from reef and more open water habitat exploitation in phase 1, a significant increase in exploitation of rocky, intertidal zones in phase 2 and significantly, the first appearance of lagoon/seagrass habitat exploitation (Diadematidae urchins) at the earliest levels of phase 3 (Kaharudin, 2020), corresponding with the emergence of a sheltered bay at this time. Whether population increase at Makpan forced an increase in diet breadth, or alternatively that access to this greater diversity of resources enabled the increase in occupation at the site, cannot be determined at this stage. However, the shell midden assemblage at Makpan accumulated due to subsistence strategies that relied on both the sheltered bay to the west and more exposed, rocky shores, reefs, and deeper waters off the south coast of Alor.

The decline in occupation intensity at the end of phase 3 and during the Early-Middle Holocene phase (P4) could be linked to continued sea level rise and the opening up of the Pantar Strait at this time, resulting in the resumption of current flow between the two islands that would have significantly impacted resource composition and collection strategies (Fig. 4). Phase 4 sees the disappearance of the Diademtidae sea urchins (Kaharudin, 2020), supporting the loss of the sheltered bay/lagoon habitat, while an increase in crab exploitation may reflect a focus on rocky shore ecosystems whose mobile, upper intertidal inhabitants are inherently more resilient to sea level changes (Kaplanis et al., 2020). Isotopic analysis of human teeth from the burial in phase 4 also suggests an increased reliance on terrestrial resources during the Middle Holocene (Roberts et al., 2020), further demonstrating the apparent negative impact these changes in coastal morphology had on the maritime subsistence strategies of Makpan's inhabitants. Our palaeogeographic reconstructions and sea level and uplift modelling, in comparison with our archaeological assemblage, suggests a coupling between site use at Makpan and local geomorphic coastal adjustments to sea-level rise.

Trends in occupation intensity and major subsistence strategies at Makpan indicate a focus on marine resources throughout. Sporadic occupation during the initial occupation phase (P1) is focused on urchins and barnacles. Intensive sea urchin exploitation is also seen during the initial occupation phase at Here Sorot Entapa, Kisar, perhaps representing a colonising strategy targeting predictable and easily collected resources (Kaharudin et al., 2019; O'Connor et al., 2019). Sea urchin and barnacle exploitation continues into phase 2 at the Pleistocene-Holocene transition, when occupation intensity increases dramatically, followed by a shift to intensive shellfish and fish predation (P3). This coincides with increased manufacture of fishhooks, a technology also observed at ca. 12 ka in a burial from nearby Tron Bon Lei (O'Connor et al., 2011b). Shell fishhooks appear from ca. 15 ka on Kisar Island (O'Connor et al., 2019) to the east, and on Timor (ca. 23−16 ka) (O'Connor et al., 2011b). Although shell beads appear in the earliest phase of occupation at Makpan, the most intensive period of settlement sees the appearance of a greater number and broader range of worked beads. This extensive bead assemblage perhaps indicates an amplified role for social signalling in response to increased contact between island communities as evidenced by the obsidian exchange network between Alor, Timor, and Kisar which began at around this time (Reepmeyer et al., 2016, 2019; Shipton et al., in press).

Following phase 4, there is a major hiatus in the Makpan record

(section 3.1.2.), suggesting the site was abandoned for approximately three thousand years between ca. 7 ka and 4 ka (Fig. 8). Interestingly, this hiatus corresponds with the end of post-LGM sea-level rise (Lambeck and Chappell, 2001), a period when relative sea level appears to have been higher than the present (Fig. 9). In view of Makpan's elevation this is unlikely to have directly impacted habitability of the cave. However, changes to nearby coastal ecosystems due to an increase in the strength of current flow through the Pantar Strait may have made Makpan less favourable (or other sites more favourable) for occupation. Future archaeological research across Alor island could clarify this issue.

The major hiatus between phases 4 and 5, beginning ca. 7 ka, has some parallels with other sites across the Wallacean region. Rising sea levels resulted in changing coastlines, and the locations, productivity, and variety of near shore habitats, impacting sites in both negative and beneficial ways (O'Connor and Chappell, 2003). Here Sorot Entapa on Kisar, Liang Sarru in the Talauds, Kelo 2 and Kelo 6 on Obi Island, and Golo Cave on Gebe Island were all abandoned in the early Holocene and only reoccupied in the mid or late Holocene (O'Connor et al., 2019; Shipton et al., 2020; Bellwood et al., 1998; Tanudirjo, 2001; Ono et al., 2009). On the other hand, neighbouring Tron Bon Lei, and Asitau Kuru on Timor, have dense occupation deposits spanning this period (Shipton et al., 2019, in press; Maloney et al., 2018b; Samper Carro et al., 2016a, 2017). Understanding to what degree these patterns reflect local or regional reorganisation of groups in the coastal landscape or simply the limited archaeological sampling across this vast archipelago will require further research.

Reoccupation of Makpan in the Neolithic likely corresponds to Late Holocene sea-level stabilisation as well as changing technologies and subsistence strategies evidenced by the appearance of pottery and domestic animals. This reoccupation phase signals a major change in the use of the cave and subsistence economies more generally. There is a significant decrease in fish and shellfish remains associated with Neolithic occupation indicating more occasional use of the site. Less intense and more sporadic site use during this time is also indicated by the increase in microvertebrates, likely the result of re-occupation of Makpan by barn owls. The slight increase in crab remains during phase 5 may be in part related to the stabilisation of sea levels at the end of the Holocene and the formation of more protected near shore environments.

5. Conclusion

The Makpan record fills a major gap in the story of MIS 3 to MIS 1 human occupation in southern Wallacea. The site demonstrates marine subsistence from the outset, with an unusual emphasis on sea urchin in the Pleistocene, perhaps reflecting the impact of human arrival on these sessile creatures. At the terminal Pleistocene there is intensification in the quantity and range of taxa exploited, as well as the first appearance of fishhook technology and an increase in the variety of shell bead types. Intensification in marine exploitation is documented elsewhere in Wallacea at this time, and the Makpan site shares the same range of marine technology and beads found on other nearby islands suggesting inter-island contact began or accelerated at this time. Terminal Pleistocene inter-island contact between distinct coastal communities has also been suggested for Alor, Kisar, and the eastern tip of Timor-Leste, based on obsidian from a single as yet unlocated source which was found in the archaeological assemblages of all three islands (Reepmeyer et al., 2019; Shipton et al., in press).

As the land bridge connecting Alor and Pantar was breached in the early Holocene, the local marine environment and its intensive exploitation at Makpan appear to have been disrupted. Occupation

continued until sea level reached a high stand ca. 7 ka, at which time the site was abandoned, perhaps because the strong current flowing through the strait was less conducive to a productive nearshore environment (or at least one which the inhabitants of Makpan had the capacity to exploit). The site was finally reoccupied in the Neolithic, when pottery was introduced and there was more of an emphasis on crabs, which may have flourished on the exposed, rocky foreshore. Makpan thus presents a 40,000-year record of maritime human subsistence, with innovative responses to significant changes in the coastline over that period, including most strikingly an intensification at the Pleistocene-Holocene transition.

Author contribution

Shimona Kealy: Writing − original draft; Data curation; Visualization; Methodology; Investigation, **Sue O'Connor:** Conceptualization; Project administration; Funding acquisition; Writing − original draft; Investigation; Supervision, **Mahirta:** Project administration; Resources; Supervision; Investigation, **Devi Mustika Sari:** Investigation; Data curation, **Ceri Shipton:** Investigation; Visualisation; Writing − review & editing, **Michelle C. Langley:** Investigation; Visualisation; Writing − review & editing, **Clara Boulanger:** Investigation, **Hendri A. F. Kaharudin:** Investigation, **Esa Putra Bayu:** Investigation, **Muhammad Abizar Algifary:** Investigation, **Abdillah Irfan:** Investigation, **Phillip Beaumont:** Investigation, **Nathan Jankowski:** Formal analysis, **Stuart Hawkins:** Investigation, **Julien Louys:** Investigation; Writing − review & editing.

Declaration of competing interest

The authors declare that they have no known competing financial interests or personal relationships that could have appeared to influence the work reported in this paper.

Acknowledgments

Appendix A. Supplementary data

Supplementary data to this article can be found online at https://doi.org/10.1016/j.quascirev.2020.106599.

References

Allen, J., O'Connell, J.F., 2008. Getting from Sunda to Sahul. In: Clark, G.R., O'Connor, S., Leach, B.F. (Eds.), Islands of Inquiry: Colonisation, Seafaring and the Archaeology of Maritime Landscapes. Terra Australis 29. ANU E Press, Canberra, Australia, pp. 31−46.

Astiduari, I.G.A.P.P., Rasyiid, T.H.A., Nugraheni, I.R., 2018. Study of coastal flooding in Kupang, east Nusa Tenggara due to tropical cyclone frances (case study April 27th − 30th 2017). IOP Conf. Ser. Earth Environ. Sci. 162 (1), 012013 https://

doi.org/10.1088/1755-1315/162/1/012013.

Ayers, J.M., Strutton, P.G., Coles, V.J., Hood, R.R., Matear, R.J., 2014. Indonesian throughflow nutrient fluxes and their potential impact on Indian Ocean productivity. Geophys. Res. Lett. 41 (14), 5060–5067. https://doi.org/10.1002/2014GL060593.

Bellwood, P., Nitihaminoto, G., Irwin, G., Gunadi, A.W., Tanudirjo, D., 1998. 35,000 years of prehistory in the northern Moluccas. In: Bartstra, G.-J. (Ed.), Bird's Head Approaches: Irian Jaya Studies, a Programme for Interdisciplinary Research. Balkema, Rotterdam, pp. 233–275.

Bird, M.I., Condie, S.A., O'Connor, S., O'Grady, D., Reepmeyer, C., Ulm, S., Zega, M., Saltré, F., Bradshaw, C.J., 2019. Early human settlement of Sahul was not an accident. Sci. Rep. 9, 8220. https://doi.org/10.1038/s41598-019-42946-9.

Bird, M.I., Turney, C.S.M., Fifield, L.K., Jones, R., Ayliffe, L.K., Palmer, A., Cresswell, R., Robertson, S., 2002. Radiocarbon analysis of the early archaeological site of Nauwalabila I, Arnhem Land, Australia: implications for sample suitability and stratigraphic integrity. Quat. Sci. Rev. 21 (8–9), 1061–1075. https://doi.org/10.1016/S0277-3791(01)00058-0.

Bowler, J.M., Johnston, H., Olley, J.M., Prescott, J.R., Roberts, R.G., Shawcross, W., Spooner, N.A., 2003. New ages for human occupation and climatic change at Lake Mungo, Australia. Nat 421 (6925), 837–840. https://doi.org/10.1038/nature01383.

Bradshaw, C.J., Ulm, S., Williams, A.N., Bird, M.I., Roberts, R.G., Jacobs, Z., Laviano, F., Weyrich, L.S., Friedrich, T., Norman, K., Saltré, F., 2019. Minimum founding populations for the first peopling of Sahul. Nat. Ecol. Evol. 3, 1057–1063. https://doi.org/10.1038/s41559-019-0902-6.

Bulbeck, D., O'Connor, S., Fakhri, Fenner, J., Marwick, B., Suryatman, Aziz, F., Hakin, B., Wibowo, U., 2019. Patterned and plain baked clay from pre-pottery contexts in Southeast Sulawesi, Indonesia. Antiquity 93 (371), 1284–1302. https://doi.org/10.15184/aqy.2019.134.

Burroughs, W.J., 2005. Climate Change in Prehistory: the End of the Reign of Chaos. Cambridge University Press, Cambridge.

Clark, J.T., 1991. Early settlement in the Indo-Pacific. J. Anthropol. Archaeol. 10 (1), 27–53. https://doi.org/10.1016/0278-4165(91)90020-X.

Clarkson, C., Jacobs, Z., Marwick, B., Fullagar, R., Wallis, L., Smith, M., Roberts, R.G., Hayes, E., Lowe, K., Carah, X., Florin, S.A., McNeil, J., Cox, D., Arnold, L.J., Hua, Q., Huntley, J., Brand, H.E.A., Manne, T., Fairbairn, A., Shulmeister, J., Lyle, L., Salinas, M., Page, M., Connell, K., Park, G., Norman, K., Murphy, T., Pardoe, C., 2017. Human occupation of northern Australia by 65,000 years ago. Nat 547, 306–310. https://doi.org/10.1038/nature22968.

Cox, N.L., 2009. Variable Uplift from Quaternary Folding along the Northern Coast of East Timor, Based on U-Series Age Determinations of Coral Terraces. PhD Thesis. Brigham Young University, Provo.

Delannoy, J.-J., David, B., Geneste, J.-M., Katherine, M., Sadier, B., Gunn, R., 2017. Engineers of the Arnhem Land Plateau: Evidence for the origins and transformation of sheltered spaces at Nawarla Gabarnmang. In: David, B., Taçon, P.S.C., Delannoy, J.-J., Geneste, J.-M. (Eds.), The Archaeology of Rock Art in Western Arnhem Land, Australia, Terra Australis, vol. 47. ANU Press, Canberra, pp. 197–244.

Fitzpatrick, S.M., Thompson, V.D., Poteate, A.S., Napolitano, M.F., Erlandson, J.M., 2016. Marginalization of the margins: the importance of smaller islands in human prehistory. J. Isl. Coast. Archaeol 11 (2), 155–170. https://doi.org/10.1080/15564894.2016.1192568.

Hawkins, S., O'Connor, S., Maloney, T.R., Litster, M., Kealy, S., Fenner, J.N., Aplin, K., Boulanger, C., Brockwell, S., Willan, R., Piotto, E., Louys, J., 2017. Oldest human occupation of Wallacea at Laili Cave, Timor-Leste, shows broad-spectrum foraging responses to late Pleistocene environments. Quat. Sci. Rev. 171, 58–72. https://doi.org/10.1016/j.quascirev.2017.07.008.

Hamm, G., Mitchell, P., Arnold, L.J., Prideaux, G.J., Questiaux, D., Spooner, N.A., Levchenko, V.A., Foley, E.C., Worthy, T.H., Stephenson, B., Coulthard, V., Coulthard, C., Wilton, S., Johnston, D., 2016. Cultural innovation and megafauna interaction in the early settlement of arid Australia. Nat 539 (7628), 280–283. https://doi.org/10.1038/nature20125.

Hantoro, W.S., Pirazzoli, P.A., Jouannic, C., Faure, H., Hoang, C.T., Radtke, U., Causse, C., Best, M.B., Lafont, R., Bieda, S., Lambeck, K., 1994. Quaternary uplifted coral reef terraces on Alor Island, East Indonesia. Coral Reefs 13 (4), 215–223. https://doi.org/10.1007/BF00303634.

Hawkins, S., Samper Carro, S.C., Louys, J., Aplin, K., O'Connor, S., Mahirta, 2018. Human palaeoecological interactions and owl roosting at Tron Bon Lei, Alor Island, Eastern Indonesia. J. Isl. Coast. Archaeol. 13 (3), 371–387. https://doi.org/10.1080/15564894.2017.1285834.

Heaton, T.J., Köhler, P., Butzin, M., Bard, E., Reimer, R.W., Austin, W.E., Ramsey, C.B., Grootes, P.M., Hughen, K.A., Kromer, B., Reimer, P.J., Adkins, J., Burke, A., Cook, M.S., Olsen, J., Skinner, L.C., 2020. Marine20—the marine radiocarbon age calibration curve (0–55,000 cal BP). Radiocarbon 1–42. https://doi.org/10.1017/RDC.2020.68.

Janßen, A., Wizemann, A., Klicpera, A., Satari, D.Y., Westphal, H., Mann, T., 2017. Sediment composition and facies of coral reef islands in the Spermonde Archipelago, Indonesia. Front. Mar. Sci. 4, 144. https://doi.org/10.3389/fmars.2017.00144.

Kaharudin, H.A.F., 2020. Prehistoric Fast Food: Sea Urchin Exploitation on Alor Island in the Pleistocene and Holocene. Masters Thesis. The Australian National University, Canberra.

Kaharudin, H.A.F., Mahirta, M., Kealy, S., Hawkins, S., Boulanger, C., O'Connor, S., 2019. Human foraging responses to climate change; Here Sorot Entapa rock-shelter on Kisar Island. Wacana 20 (3), 525–559. https://doi.org/10.17510/

wacana.v20i3.783.

Kaplanis, N.J., Edwards, C.B., Eynaud, Y., Smith, J.E., 2020. Future sea-level rise drives rocky intertidal habitat loss and benthic community change. PeerJ 8, e9186. https://doi.org/10.7717/peerj.9186.

Kealy, S., Louys, J., O'Connor, S., 2016. Islands under the sea: a review of early modern human dispersal routes and migration hypotheses through Wallacea. J. Isl. Coast. Archaeol. 11 (3), 364–384. https://doi.org/10.1080/15564894.2015.1119218.

Kealy, S., Louys, J., O'Connor, S., 2017. Reconstructing palaeogeography and inter-island visibility in the Wallacean Archipelago during the likely period of Sahul colonization, 65–45 000 years ago. Archaeol. Prospect. 24 (3), 259–272. https://doi.org/10.1002/arp.1570.

Kealy, S., Louys, J., O'Connor, S., 2018. Least-cost pathway models indicate northern human dispersal from Sunda to Sahul. J. Hum. Evol. 125, 59–70. https://doi.org/10.1016/j.jhevol.2018.10.003.

Koesoemadinata, S., Noya, N., 1989. Peta Geologi Lembar Lomblen, Nusatenggara Timur. Pusat Penelitian dan Pengembangan Geologi, Bandung.

Lambeck, K., Chappell, J., 2001. Sea level change through the last glacial cycle. Science 292 (5517), 679–686. https://doi.org/10.1126/science.1059549.

Langley, M.C., O'Connor, S., Kealy, S., Mahirta, 2020. Fishhooks, lures, and sinkers: intensive manufacture of marine technology from the terminal Pleistocene at Makpan cave, Alor island, Indonesia. J. Isl. Coast. Archaeol. In press.

Lawrence, J.M., 2007. Edible sea urchins: use and life-history strategies. In: Lawrence, J.M. (Ed.), Developments in Aquaculture and Fisheries Science, second ed., vol. 37. Elsevier, Amsterdam, The Netherlands, pp. 1–9. https://doi.org/10.1016/S0167-9309(07)80065-2. Edible Sea Urchins: Biology and Ecology.

Louys, J., Kealy, S., O'Connor, S., Price, G.J., Hawkins, S., Aplin, K., Rizal, Y., Zaim, J., Tanudirjo, D.A., Santoso, W.D., Hidayah, A.R., Trihascaryo, A., Wood, R., Bevitt, J., Clark, T., 2017. Differential preservation of vertebrates in Southeast Asian caves. Int. J. Speleol. 46 (3), 379–408. https://doi.org/10.5038/1827-806X.46.3.2131.

Louys, J., O'Connor, S., Higgins, P., Hawkins, S., Maloney, T., 2018. New genus and species of giant rat from Alor Island, Indonesia. J. Asia-Pacific Biodivers. 11 (4), 503–510. https://doi.org/10.1016/j.japb.2018.08.005.

Major, J., Harris, R., Chiang, H.W., Cox, N., Shen, C.C., Nelson, S.T., Prasetyadi, C., Rianto, A., 2013. Quaternary hinterland evolution of the active Banda Arc: surface uplift and neotectonic deformation recorded by coral terraces at Kisar, Indonesia. J. Asian Earth Sci. 73, 149–161. https://doi.org/10.1016/j.jseaes.2013.04.023.

Maloney, T., O'Connor, S., Wood, R., Aplin, K., Balme, J., 2018a. Carpenters Gap 1: a 47,000 year old record of indigenous adaption and innovation. Quat. Sci. Rev. 191, 204–228. https://doi.org/10.1016/j.quascirev.2018.05.016.

Maloney, T.R., O'Connor, S., Reepmeyer, C., 2018b. Specialised lithic technology of terminal Pleistocene maritime peoples of Wallacea. Archaeol. Res. Asia 16, 78–87. https://doi.org/10.1016/j.ara.2018.05.003.

Morton, R.A., Gelfenbaum, G., Jaffe, B.E., 2007. Physical criteria for distinguishing sandy tsunami and storm deposits using modern examples. Sediment. Geol. 200 (3–4), 184–207. https://doi.org/10.1016/j.sedgeo.2007.01.003.

Morwood, M.J., Sutikna, T., Saptomo, E.W., Hobbs, D.R., Westaway, K.E., 2009. Preface: research at Liang Bua, Flores, Indonesia. J. Hum. Evol. 57 (5), 437–449. https://doi.org/10.1016/j.jhevol.2009.07.003.

Norman, K., Inglis, J., Clarkson, C., Faith, J.T., Shulmeister, J., Harris, D., 2018. An early colonisation pathway into northwest Australia 70-60,000 years ago. Quat. Sci. Rev. 180, 229–239. https://doi.org/10.1016/j.quascirev.2017.11.023.

Nott, J., Green, C., Townsend, I., Callaghan, J., 2014. The world record storm surge and the most intense Southern Hemisphere tropical cyclone: new evidence and modeling. Bull. Am. Meteorol. Soc. 95 (5), 757–765. https://doi.org/10.1175/BAMS-D-12-00233.1.

Obuch, J., Benda, P., 2009. Food of the barn owl (*Tyto alba*) in the eastern mediterranean. Slovak Rapt. J. 3 (1), 41–50.

O'Connell, J.F., Allen, J., 2012. The restaurant at the end of the universe: modelling the colonisation of Sahul. Aust. Archaeol. 74, 5–17. https://www.jstor.org/stable/23621508.

O'Connor, S., Barham, A., Aplin, K., Dobney, K., Fairbairn, A., Richards, M., 2011a. The power of paradigms: examining the evidential basis for early to mid-Holocene pigs and pottery in Melanesia. J. Pac. Archaeol. 2 (2), 1–25. https://pacificarchaeology.org/index.php/journal/article/view/56.

O'Connor, S., Chappell, J., 2003. Colonisation and coastal subsistence in Australia and Papua New Guinea: different timing, different modes. In: Sand, C. (Ed.), Pacific Archaeology: Assessments and Prospects. Proceedings of the International Conference for the 50th Anniversary of the First Lapita Excavation (July 1952), Koné-Nouméa 2002. Le Cahiers de l'Archéologie en Nouvelle-Calédonie, Nouméa, pp. 17–32.

O'Connor, S., Louys, J., Kealy, S., Samper Carro, S.C., 2017a. Hominin dispersal and settlement east of Huxley's Line: the role of sea level changes, island size, and subsistence behavior. Curr. Anthropol. 58 (S17), S567–S582. https://doi.org/10.1086/694252.

O'Connor, S., Mahirta, Kealy, S., Boulanger, C., Maloney, T., Hawkins, S., Langley, M.C., Kaharudin, H.A., Suniarti, Y., Husni, M., Ririmasse, M., Tanudirjo, D.A., Wattimena, L., Handoko, W., Alifah, Louys, J., 2019. Kisar and the archaeology of small islands in the Wallacean Archipelago. J. Isl. Coast. Archaeol. 14 (2), 198–225. https://doi.org/10.1080/15564894.2018.1443171.

O'Connor, S., Ono, R., Clarkson, C., 2011b. Pelagic fishing at 42,000 years before the present and the maritime skills of modern humans. Sci 334 (6059), 1117–1121. https://doi.org/10.1126/science.1207703.

O'Connor, S., Samper Carro, S.C., Hawkins, S., Kealy, S., Louys, J., Wood, R., 2017b.

Fishing in life and death: Pleistocene fish-hooks from a burial context on Alor Island, Indonesia. Antiquity 91 (360), 1451–1468. https://doi.org/10.15184/aqy.2017.186.

Ono, R., 2010. Ethno-archaeology and early Austronesian fishing strategies in near-shore environments. J. Polyn. Soc. 119 (3), 269–314.

Ono, R., Soegondho, S., Yoneda, M., 2009. Changing marine exploitation during late Pleistocene in Northern Wallacea: shell remains from Leang Sarru rockshelter in Talaud Islands. Asian Perspect. 48, 318–341. https://www.jstor.org/stable/42928767.

Pedoja, K., Husson, L., Johnson, M.E., Melnick, D., Witt, C., Pochat, S., Nexer, M., Delcaillau, B., Pinegina, T., Poprawski, Y., Authemayou, C., 2014. Coastal staircase sequences reflecting sea-level oscillations and tectonic uplift during the Quaternary and Neogene. Earth Sci. Rev. 132, 13–38. https://doi.org/10.1016/j.earscirev.2014.01.007.

Phantuwongraj, S., Choowong, M., 2012. Tsunamis versus storm deposits from Thailand. Nat. Hazards 63 (1), 31–50. https://doi.org/10.1007/s11069-011-9717-8.

Ramsey, C.B., 2017. Methods for summarizing radiocarbon datasets. Radiocarbon 59 (6), 1809–1833. https://doi.org/10.1017/RDC.2017.108.

Ramsey, C.B., 2009a. Bayesian analysis of radiocarbon dates. Radiocarbon 51 (1), 337–360. https://doi.org/10.1017/S0033822200033865.

Ramsey, C.B., 2009b. Dealing with outliers and offsets in radiocarbon dating. Radiocarbon 51 (3), 1023–1045. https://doi.org/10.1017/S0033822200034093.

Reepmeyer, C, O'Connor, S, Mahirta, Kealy, S, Maloney, T, 2019. Kisar, a small island participant in an extensive maritime obsidian network in the Wallacean Archipelago. Archaeol. Res. Asia 19, 100139. https://doi.org/10.1016/j.ara.2019.100139.

Reepmeyer, C., O'Connor, S., Mahirta, Maloney, T., Kealy, S., 2016. Late pleistocene/early holocene maritime interaction in Southeastern Indonesia − Timor Leste. J. Archaeol. Sci. 76, 21–30. https://doi.org/10.1016/j.jas.2016.10.007.

Reimer, P.J., Austin, W.E., Bard, E., Bayliss, A., Blackwell, P.G., Ramsey, C.B., Butzin, M., Cheng, H., Edwards, R.L., Friedrich, M., Grootes, P.M., et al., 2020. The IntCal20 Northern Hemisphere radiocarbon age calibration curve (0−55 cal kBP). Radiocarbon 1–33. https://doi.org/10.1017/RDC.2020.41.

Roberts, P., Louys, J., Zech, J., Shipton, C., Kealy, S., Samper Carro, S., Hawkins, S., Boulanger, C., Marzo, S., Fiedler, B., Boivin, N., Mahirta, Aplin, K., O'Connor, S., 2020. Isotopic evidence for initial coastal colonization and subsequent diversification in the human occupation of Wallacea. Nat. Commun. 11 (1), 1–11. https://doi.org/10.1038/s41467-020-15969-4.

Romano, A., Séchaud, R., Roulin, A., 2020. Global biogeographical patterns in the diet of a cosmopolitan avian predator. J. Biogeogr. 47, 1467–1481. https://doi.org/10.1111/jbi.13829.

Roosmawati, N., Harris, R., 2009. Surface uplift history of the incipient Banda arc-continent collision: geology and synorogenic foraminifera of Rote and Savu Islands, Indonesia. Tectonophysics 479 (1−2), 95–110. https://doi.org/10.1016/j.tecto.2009.04.009.

Samper Carro, S.C., Gilbert, F., Bulbeck, D., O'Connor, S., Louys, J., Spooner, N., Questiaux, D., Arnold, L., Price, G.J., Wood, R., Mahirta, 2019. Somewhere beyond the sea: human cranial remains from the Lesser Sunda Islands (Alor Island, Indonesia) provide insights on Late Pleistocene peopling of Island Southeast Asia. J. Hum. Evol. 134, 102638. https://doi.org/10.1016/j.jhevol.2019.07.002.

Samper Carro, S.C., Louys, J., O'Connor, S., 2017. Methodological considerations for icthyoarchaeology from the Tron Bon Lei sequence, Alor, Indonesia. Archaeol. Res. Asia 12, 11–22. https://doi.org/10.1016/j.ara.2017.09.006.

Samper Carro, S.C., Stewart, T.J, Mahirta, Wood, R., O'Connor, S., (forthcoming). Burial practices in the early mid-Holocene of the Wallacean Islands: a sub-adult burial from Gua Makpan, Alor Island, Indonesia. Quat. Int..

Samper Carro, S.C., O'Connor, S., Louys, J., Hawkins, S., Mahirta, M., 2016a. Human maritime subsistence strategies in the Lesser Sunda Islands during the terminal Pleistocene−early Holocene: new evidence from Alor, Indonesia. Quat. Int. 416, 64–79. https://doi.org/10.1016/j.quaint.2015.07.068.

Samper Carro, S.C., Louys, J., Kealy, S., O'Connor, S., 2016b. True colours: experimental study of Pacific fish bones to assess bone colouring related to burning and post-depositional processes. In: Conference Presentation at the 4th ICAZ Taphonomy Working Group, 7th - 10th September 2016.

Shen, C.C., Wu, C.C., Dai, C.F., Gong, S.Y., 2018. Variable uplift rate through time: Holocene coral reef and neotectonics of Lutao, eastern Taiwan. J. Asian Earth Sci. 156, 201–206. https://doi.org/10.1016/j.jseaes.2018.01.016.

Shipton, C., Kealy, S., Mahirta, Irfan, A., Patridina, E.P.B.G.G., O'Connor, S., (forthcoming). Pleistocene lithic technology from Alor Island articulates with the records of Flores and Timor across southern Wallacea. PaleoAnthropology.

Shipton, C., O'Connor, S., Jankowski, N., O'Connor-Veth, J., Maloney, T., Kealy, S., Boulanger, C., 2019. A new 44,000-year sequence from Asitau Kuru (Jerimalai), Timor-Leste, indicates long-term continuity in human behaviour. Archaeol. Anthropol. Sci. 11 (10), 5717–5741. https://doi.org/10.1007/s12520-019-00840-5.

Shipton, C., O'Connor, S., Kealy, S., Mahirta, Syarqiyah, I.N., Alamsyah, N., 2020. Ground axe technology in Wallacea: the first excavations on Obi Island. PloS One 15 (8), e0236719. https://doi.org/10.1371/journal.pone.0236719.

Shipton, C., O'Connor, S., Reepmeyer, C., Kealy, S., Jankowski, N., 2020. Shell Adzes, exotic obsidian, and inter-island voyaging in the early and middle Holocene of Wallacea. J. Isl. Coast. Archaeol. https://doi.org/10.1080/15564894.2019.1581306. In press.

Smith, W.H., Sandwell, D.T., 1997. Global sea floor topography from satellite altimetry and ship depth soundings. Sci 277 (5334), 1956–1962. https://doi.org/10.1126/science.277.5334.1956.

Southon, J., Kashgarian, M., Fontugne, M., Metivier, B., Yim, W.W., 2002. Marine reservoir corrections for the Indian Ocean and Southeast Asia. Radiocarbon 44 (1), 167–180. https://doi.org/10.1017/S0033822200064778.

Spriggs, M., 1996. Chronology and colonisation on Island Southeast Asia and the Pacific: New data and an evaluation. In: Davidson, J.M., Irwin, G., Leach, B.F., Pawley, A., Brown, D. (Eds.), Oceanic Culture History: Essays in Honour of Roger Green. New Zealand Journal of Archaeology Special Publications, Auckland, pp. 33−55.

Sutikna, T., Tocheri, M.W., Faith, J.T., Awe, R.D., Meijer, H.J., Saptomo, E.W., Roberts, R.G., 2018. The spatio-temporal distribution of archaeological and faunal finds at Liang Bua (Flores, Indonesia) in light of the revised chronology for *Homo floresiensis*. J. Hum. Evol. 124, 52–74. https://doi.org/10.1016/j.jhevol.2018.07.001.

Szabó, K., Amesbury, J.R., 2011. Molluscs in a world of islands: the use of shellfish as a food resource in the tropical island Asia-Pacific region. Quat. Int. 239 (1−2), 8–18. https://doi.org/10.1016/j.quaint.2011.02.033.

Tanudirjo, D.A., 2001. Islands in between: Prehistory of the Northeastern Indonesian Archipelago. PhD Thesis. Australian National University, Canberra.

Tobler, R., Rohrlach, A., Soubrier, J., Bover, P., Llamas, B., Tuke, J., Bean, N., Abdullah-Highfold, A., Agius, s., O'Donoghue, A., O'Loughlin, I., Sutton, P., Zilio, F., Walshe, K., Williams, A.N., Turney, C.S.M., Williams, M., Richards, S.M., Mitchell, R.J., Kowal, E., Stephen, J.R., Williams, L., Haak, W., Cooper, A., 2017. Aboriginal mitogenomes reveal 50,000 years of regionalism in Australia. Nat 544 (7649), 180–184. https://doi.org/10.1038/nature21416.

Tucker, M.E., 2001. Sedimentary Petrology: an Introduction to the Origin of Sedimentary Rocks, third ed. Blackwell Publishing, Oxford, UK.

Turney, C.S., Bird, M.I., Fifield, L.K., Roberts, R.G., Smith, M., Dortch, C.E., Grün, R., Lawson, E., Ayliffe, L.K., Miller, G.H., Dortch, J., Cresswell, R.G., 2001. Early human occupation at Devil's Lair, southwestern Australia 50,000 years ago. Quat. Res. 55 (1), 3–13. https://doi.org/10.1006/qres.2000.2195.

Vandenberghe, J., 2013. Grain size of fine-grained windblown sediment: a powerful proxy for process identification. Earth Sci. Rev. 121, 18−30. https://doi.org/10.1016/j.earscirev.2013.03.001.

Veth, P., Ward, I., Manne, T., Ulm, S., Ditchfield, K., Dortch, J., Hook, F., Petchey, F., Hogg, A., Questiaux, D., Demuro, M., Arnold, L., Spooner, N., Levchenko, V., Skippington, J., Byrne, C., Basgall, M., Zeanah, D., Belton, D., Helmholz, P., Bajkan, S., Bailey, R., Placzek, C., Kendrick, P., 2017. Early human occupation of a maritime desert, Barrow Island, North-West Australia. Quat. Sci. Rev. 168, 19−29. https://doi.org/10.1016/j.quascirev.2017.05.002.

Wood, R., Jacobs, Z., Vannieuwenhuyse, D., Balme, J., O'Connor, S., Whitau, R., 2016. Towards an accurate and precise chronology for the colonization of Australia: the example of Riwi, Kimberley, Western Australia. PloS One 11 (9), e0160123. https://doi.org/10.1371/journal.pone.0160123.